Hydrogen Electrolyzer Flow Distributor Model

M. A. Shadday

September 2006

SRNL
SAVANNAH RIVER NATIONAL LABORATORY
TM

DISCLAIMER

This report was prepared by Washington Savannah River Company (WSRC) for the United States Department of Energy under Contract No. DE-AC09-96SR18500 and is an account of work performed under that contract. Neither the United States Department of Energy, nor WSRC, nor any of their employees makes any warranty, expressed or implied, or assumes any legal liability or responsibility for the accuracy, completeness, or usefulness, of any information, apparatus, or product or process disclosed herein or represents that its use will not infringe privately owned rights. Reference herein to any specific commercial product, process, or service by trademark, name, manufacturer or otherwise does not necessarily constitute or imply endorsement, recommendation, or favoring of same by WSRC or by the United States Government or any agency thereof. The views and opinions of the authors expressed herein do not necessarily state or reflect those of the United States Government or any agency thereof.

Printed in the United States of America

Prepared For
U.S. Department of Energy

Hydrogen Electrolyzer Flow Distributor Model

Savannah River National Laboratory

M. Andy Shadday

Publication Date: September 2006

DOCUMENT: WSRC-STI-2006-00133

TITLE: Hydrogen Electrolyzer Flow Distributor Model

APPROVALS

M. A. Shadday, Author (Computational & Stat. Sci. Group, SRNL)　　　9/27/06　Date

L. L. Hamm, Technical Reviewer (Computational & Stat. Sci. Group, SRNL)　　9/27/06　Date

S. J. Hensel, Manager (Computational & Stat. Sci. Group, SRNL)　　　9/22/06　Date

W. A. Summers, Principal Investigator (Energy & Security, SRNL)　　9/28/06　Date

Table of Contents

List of Figures

This Page Intentionally Left Blank

Washington Savannah River Company
Hydrogen Electrolyzer Flow Distributor Model
September 2006

WSRC-STI-2006-00133
Revision 0
Page 1 of 47

Introduction and Summary

The hybrid sulfur process (HyS) hydrogen electrolyzer consists of a proton exchange membrane (PEM) sandwiched between two porous graphite layers. An aqueous solution of sulfuric acid with dissolved SO_2 gas flows parallel to the PEM through the porous graphite layer on the anode side of the electrolyzer. A flow distributor, consisting of a number of parallel channels acting as headers, promotes uniform flow of the anolyte fluid through the porous graphite layer. A numerical model of the hydraulic behavior of the flow distributor is herein described. This model was developed to be a tool to aid the design of flow distributors. The primary design objective is to minimize spatial variations in the flow through the porous graphite layer.

The hydraulic data from electrolyzer tests consists of overall flowrate and pressure drop. Internal pressure and flow distributions are not measured, but these details are provided by the model. The model has been benchmarked against data from tests of the current electrolyzer. The model reasonably predicts the viscosity effect of changing the fluid from water to an aqueous solution of 30 % sulfuric acid. The permeability of the graphite layer was the independent variable used to fit the model to the test data, and the required permeability for a good fit is within the range literature values for carbon paper. The model predicts that reducing the number of parallel channels by 50 % will substantially improve the uniformity of the flow in the porous graphite layer, while maintaining an acceptable pressure drop across the electrolyzer. When the size of the electrolyzer is doubled from 2.75 inches square to 5.5 inches square, the same number of channels as in the current design will be adequate, but it is advisable to increase the channel cross-sectional flow area. This is due to the increased length of the channels.

Flow Distributor Description

The current flow distributor design consists of a carbon block, with parallel grooves machined in the side that is pressed against the porous graphite layer. The porous graphite layer, in which the flow is parallel to the PEM, is a sheet of carbon paper. Figure 1 shows a section of the flow distributor with three parallel flow channels (grooves) in the carbon block. The central channel acts as a supply header and the channels on either side act as exhaust headers for the anolyte flow in the carbon paper. The axial flow in both the supply and exhaust channels is in the same direction. There is a downward vertical component to the axial flow in the supply channel. This fluid enters the porous carbon paper and flows laterally towards the two adjacent exhaust channels and then upward into the channels. The axial flows decrease in the streamwise direction in the supply channels and increase in the exhaust channels.
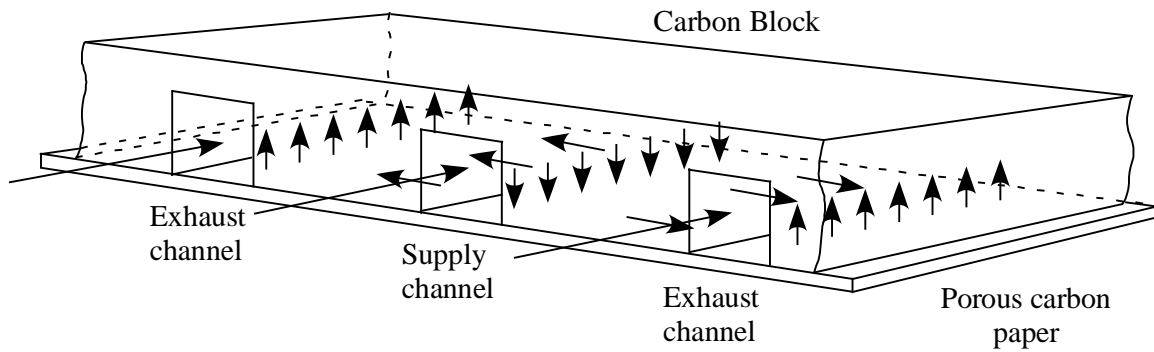
Fig. 1: A section of the electrolyzer flow distributor showing the flow pattern.

Figures 2 and 3 are drawings of the current design of the electrolyzer flow distributor. Figure 2 shows the grooves in the carbon block, and figure 3 shows the supply and exhaust headers for the flow distributor. There are thirty parallel channels, fifteen supply and fifteen exhaust. The channel dimensions are: height 0.05 inches, width 0.031 inches, and length 2.82 inches. There are headers at both ends of the electrolyzer. The flow enters the supply channels at one end from the supply header above through slots, and the flow exits the exhaust channels at the other end through slots to the exhaust header above. The porous carbon paper is 0.007 inches thick.

Washington Savannah River Company   WSRC-STI-2006-00133
Hydrogen Electrolyzer Flow Distributor Model   Revision 0
September 2006   Page 3 of 47
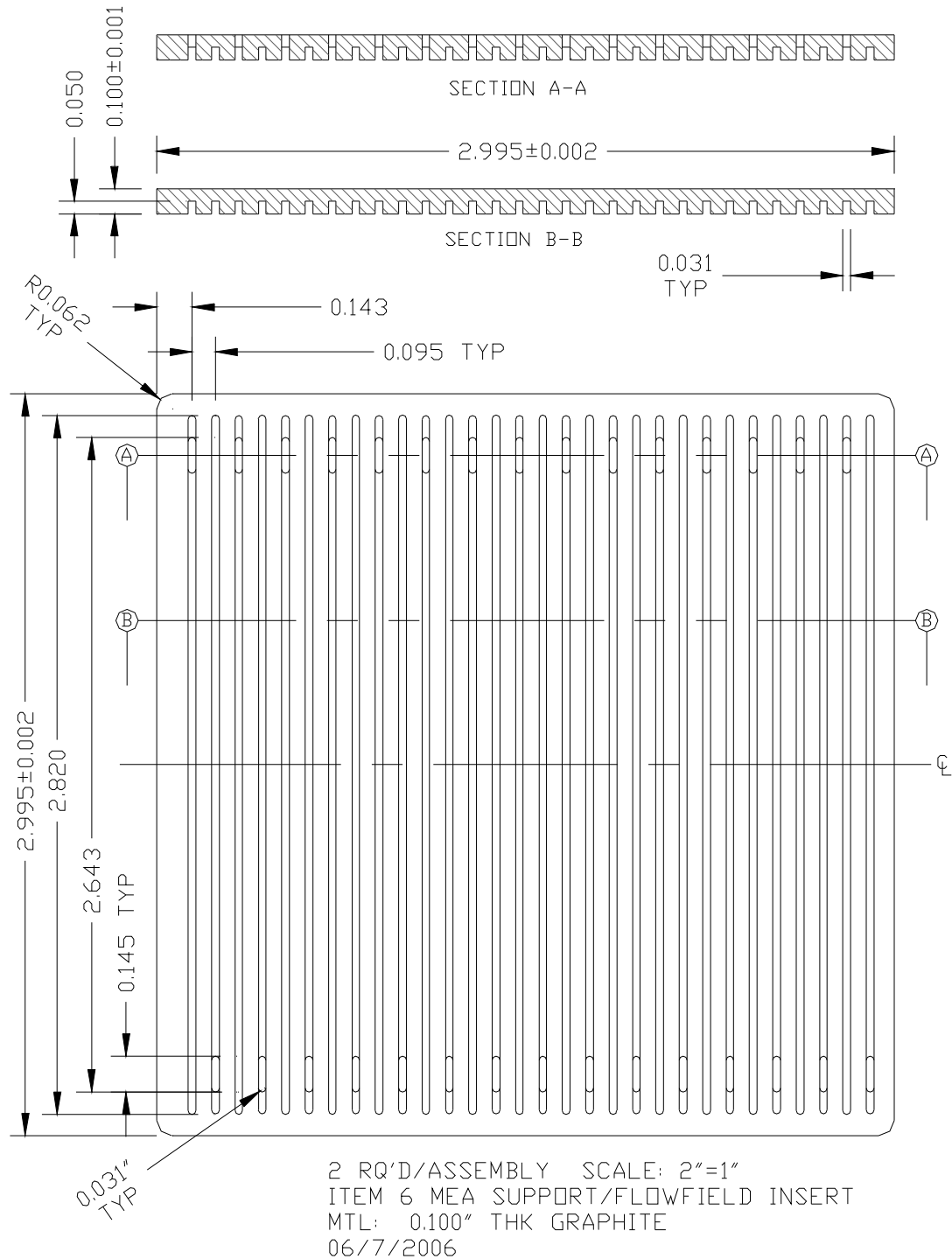
Fig. 2: Drawing of the current design flow distributor, showing the graphite block.

Washington Savannah River Company   WSRC-STI-2006-00133
Hydrogen Electrolyzer Flow Distributor Model   Revision 0
September 2006   Page 4 of 47

2.994

0.188
0.244

0.143

0.190 TYP

0.151 TYP

0.031 TYP

0.188±0.001

0.158

2 RQ'D/ASSEMBLY
SCALE: TWICE FULL SIZE
ITEM 14 TOP FLOW DISTRIBUTOR
MTL: HASTELLOY B-2
06/17/2006

2.994

0.188
0.244

0.238

0.190 TYP

0.151 TYP

0.031 TYP

0.188±0.001

0.158

2 RQ'D/ASSEMBLY
SCALE: TWICE FULL SIZE
ITEM 15 BOTTOM FLOW DISTRIBUTOR
MTL: HASTELLOY B-2
06/17/2006

Fig. 3: Drawing of the current design flow distributor, showing the supply and exhaust headers for the parallel channels.

Model Description

Figure 4 is a schematic of a flow distributor with ten channels, showing the flow pattern. The schematic also shows the discretezation of the flow network into five axial control volumes for each channel. The porous layer region between each set of adjacent channels is also divided into five control volumes. This reduced size mesh was used to develop the original flow distributor model. The architecture of the model is such that the number of channels and the axial discretezation is easily changed.

The model predicts the steady-state flow distribution in the distributor. The supply and exhaust headers are assumed to be ideal manifolds. The supply pressure is the boundary condition at the entrance to each of the supply channels, and the exhaust pressure is the

Washington Savannah River Company
Hydrogen Electrolyzer Flow Distributor Model
September 2006

WSRC-STI-2006-00133
Revision 0
Page 5 of 47

boundary condition at the effluent end of each of the exhaust channels. The lateral flows in the porous layer are assumed to be perpendicular to the channels.
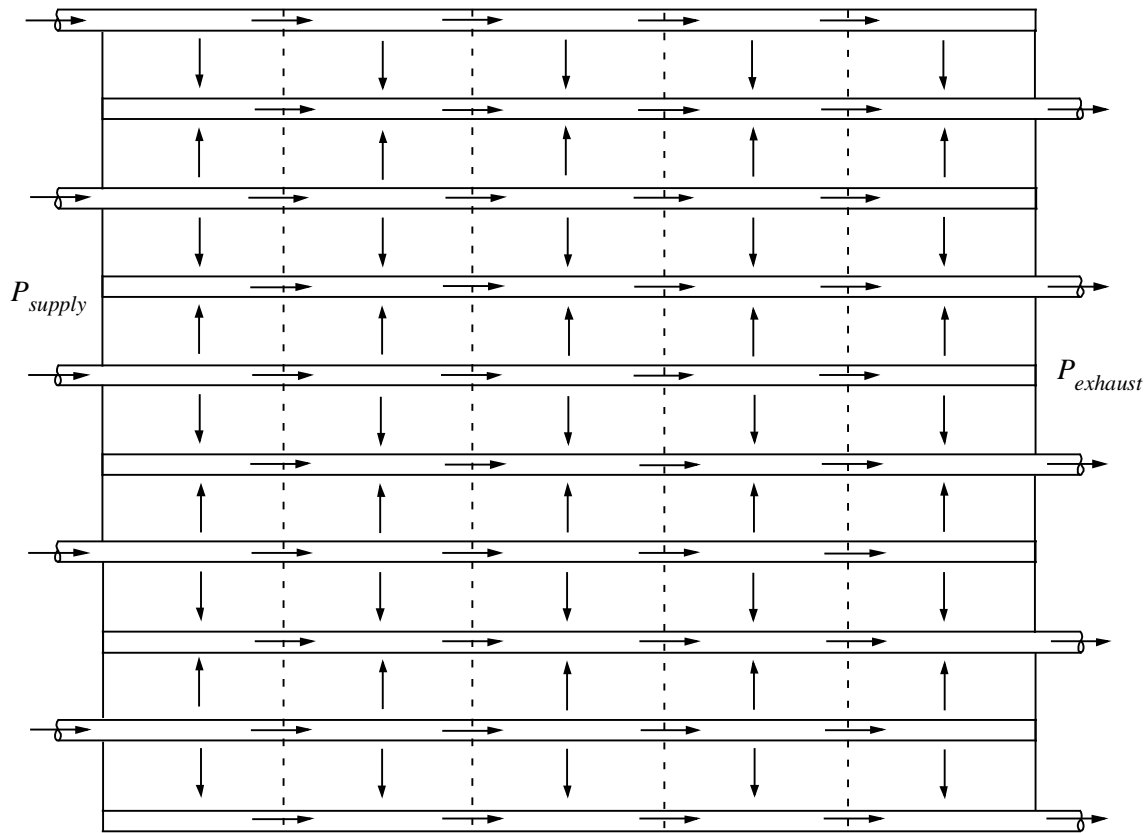
Fig. 4: Schematic of a flow distributor showing the flow pattern.

The axial flow in the supply and exhaust channels is assumed to be governed by the linear momentum equation. Figures 5 and 6 are schematics of single control volumes in the supply and exhaust channels respectively. The bottom flow into or out of the channel is assumed to be uniform over the length of the control volume. The axial flow in the channel is assumed to be laminar. Equation (1) is the momentum equation for a control volume in a supply channel, and equation (2) is the momentum equation for a control volume in an exhaust channel. These equations are derived in Appendix A.

Washington Savannah River Company
Hydrogen Electrolyzer Flow Distributor Model
September 2006

WSRC-STI-2006-00133
Revision 0
Page 6 of 47
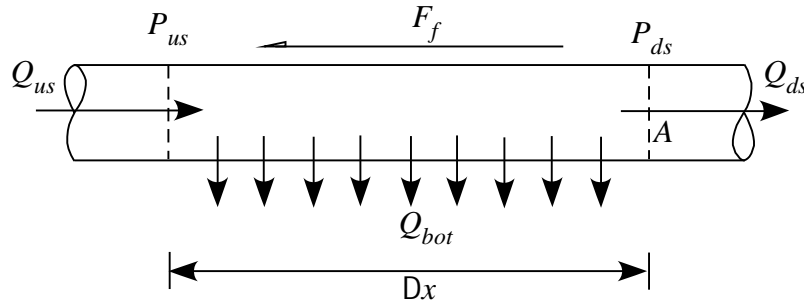
Fig. 5: Schematic of a single control volume in a supply channel.
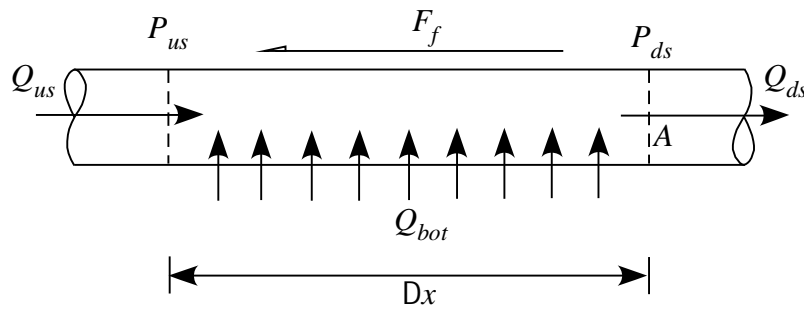
Fig. 6: Schematic of a single control volume in an exhaust channel.

$$Q_{ds}^2 + \frac{Q_{bot}}{2}(Q_{us} + Q_{ds}) - Q_{us}^2 = (P_{us} - P_{ds})\frac{A^2}{\rho} - \frac{16\mu\Delta xA}{\rho D_H^2}(Q_{us} + Q_{ds}) \qquad (1)$$

$$Q_{ds}^2 - Q_{us}^2 = (P_{us} - P_{ds})\frac{A^2}{\rho} - \frac{16\mu\Delta xA}{\rho D_H^2}(Q_{us} + Q_{ds}) \qquad (2)$$

Figure 7 is a schematic of a control volume in the porous carbon paper. The flow is assumed to be governed by the Ergun equation, [1]. Equation (3) is the momentum equation for the flow in the carbon paper. This equation is derived in Appendix A. The three momentum equations for the three types of control volumes and the two continuity equations for the channel control volumes form a set of simultaneous non-linear equations for the flow and pressure distributions in the flow distributor. This set of equations is solved iteratively by Newton's method.

Washington Savannah River Company   WSRC-STI-2006-00133
Hydrogen Electrolyzer Flow Distributor Model   Revision 0
September 2006   Page 7 of 47
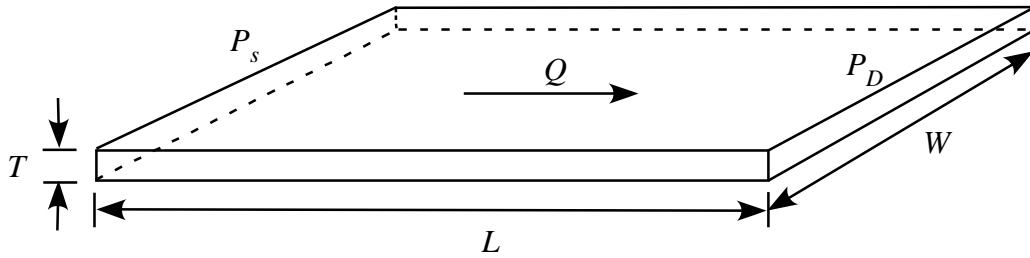
Fig. 7: Schematic of a single control volume in the porous carbon paper.

$$\left(P_{Si} + P_{Si+1}\right) - \left(P_{Di} + P_{Di+1}\right) = \frac{300\text{m}L}{AD_p^2}\frac{(1-\text{e})^2}{\text{e}^3}Q + \frac{3.5\text{r}L}{A^2 D_p}\frac{1-\text{e}}{\text{e}^3}Q^2 \tag{3}$$

The flow resistance of porous media is generally characterized by the permeability. Equation (4) is the expression used to calculate the permeability "k" from pressure drop versus flowrate data. The permeability of carbon paper is approximately 7.5×10^{-12} m^2, [2]. The Ergun equation uses two parameters, a characteristic particle diameter D_p and the interstial porosity e, to characterize the hydraulic behavior of a porous media. If the porosity is known, the permeability uniquely determines the characteristic particle diameter. The first term on the right side of the Ergun equation applies to laminar flow and is termed the Blake-Kozeny equation. The expressions for the pressure gradient in the permeability equation, equation (4), and the Blake-Kozeny equation are equated in equation (5). This expression is simplified to obtain equation (6), an expression relating the permeability, characteristic particle diameter, and porosity. A porous material with a permeability of 7.5×10^{-12} m^2 and a porosity of 0.6 has a characteristic particle diameter of 2.88×10^{-5} m.

$$Q = \frac{k}{\text{m}}\frac{\Delta P}{L}(A) \tag{4}$$

$$\frac{\Delta P}{L} = \frac{Q\text{m}}{kA} = \frac{150\text{m}Q}{AD_p^2}\frac{(1-\text{e})^2}{\text{e}^3} \tag{5}$$

$$\frac{1}{k} = \frac{150}{D_p^2}\frac{(1-\text{e})^2}{\text{e}^3} \tag{6}$$

The flow distributor of the electrolyzer currently being tested has thirty parallel channels. The model has been expanded to thirty channels and each channel is divided into ten sequential control volumes in the axial direction. The model was benchmarked against electrolyzer hydraulic test data, using both water and an aqueous solution of 30 weight percent sulfuric acid. These results are shown in figure 8. The fluid temperatures are 22.0 ºC, and the viscosities of the water and the 30 weight percent sulfuric acid solution

Washington Savannah River Company   WSRC-STI-2006-00133
Hydrogen Electrolyzer Flow Distributor Model   Revision 0
September 2006   Page 8 of 47

are respectively 1.006×10^{-3} and 2.022×10^{-3} kg/m-s. The value of the characteristic particle diameter was used to fit the data. The value used was 3.01×10^{-5} m. The fit is pretty good, and the viscosity effect is certainly captured.
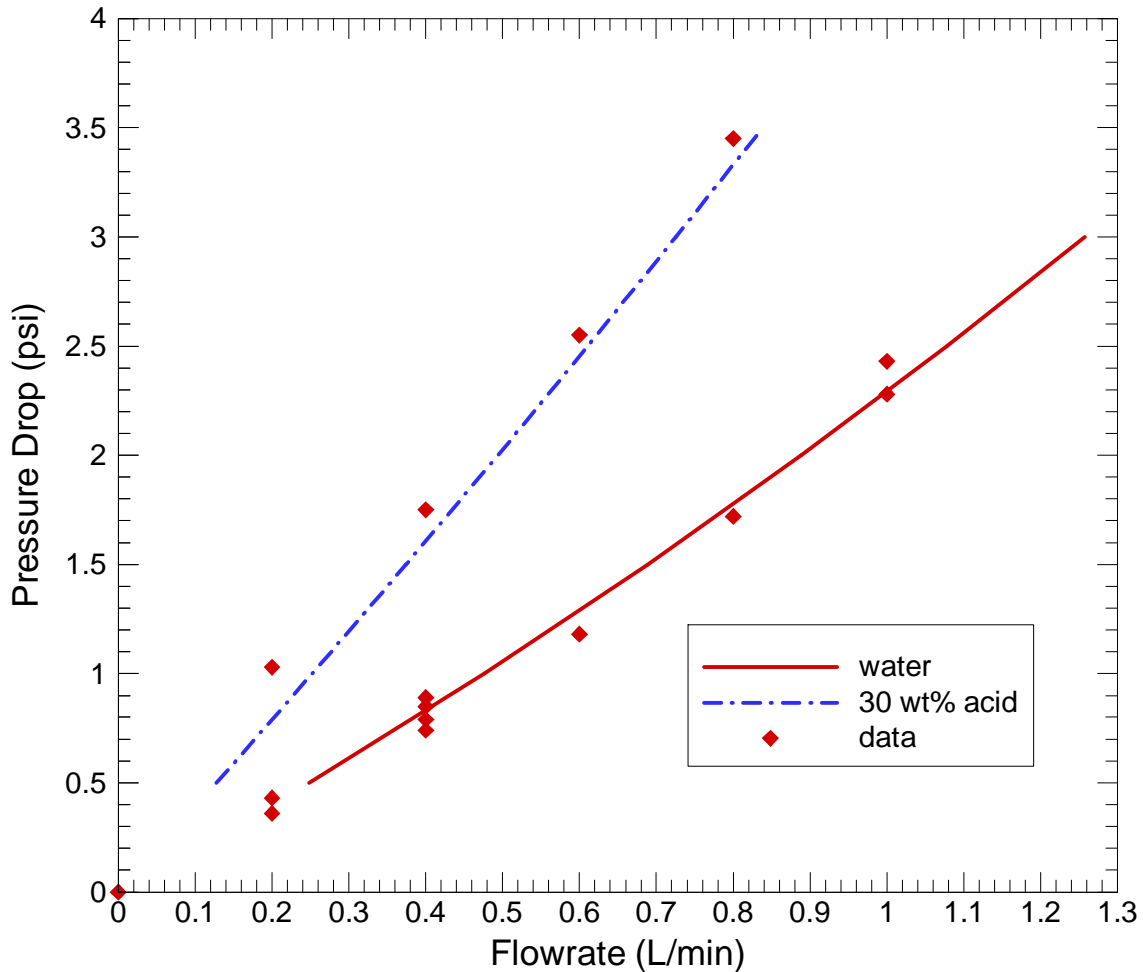
Fig. 8: Overall pressure drop versus flowrate for the test electrolyzer with two different fluids.

Internal pressures and flowrates were not measured in the electrolyzer tests, therefore test data can only be used to verify the overall hydraulic performance of the model. Aspects of the model were validated in several different ways: comparison with analytical solutions where possible, verifying that mass is conserved globally, and comparison between model results and hand calculations. Pressure profiles in the supply and exhaust channels were compared with analytical solutions. Figure 9 is a drawing of axial flow through a channel with uniform flow out through the bottom of the channel. Equation (7) is an ordinary first-order differential equation which governs this flow. Equation (8) is the solution to the differential equation and an expression for the axial pressure profile in the channel. The differential equation is derived and integrated to produce the solution in Appendix B. Figure 10 shows a comparison between model results and the analytical

Washington Savannah River Company   WSRC-STI-2006-00133
Hydrogen Electrolyzer Flow Distributor Model   Revision 0
September 2006   Page 9 of 47

solution for the axial pressure distribution in a supply channel near the center of the flow distributor. The agreement is very good. The assumed permeability of the porous layer in this case is low and the flow out the bottom of the channel is therefore close to uniform axially. Axially uniform flow out of the bottom of a channel is not an assumption in the model, and it will subsequently be demonstrated that this is generally not the case.
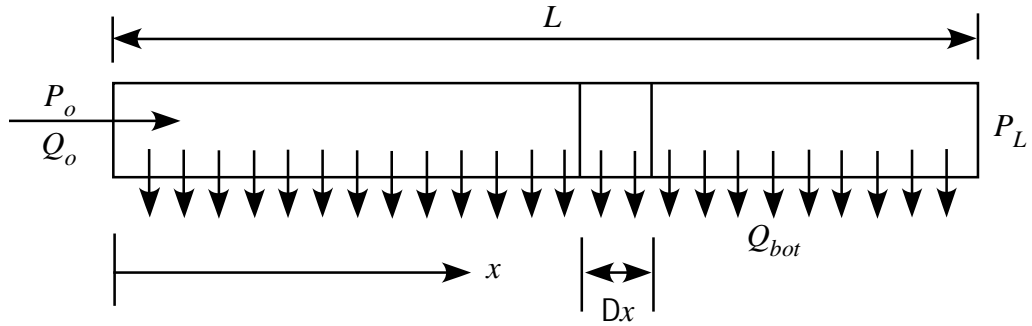
Fig. 9: Schematic of axial flow through a channel with uniform flow out through the bottom of the channel.

$$\frac{dP}{dx} = \left(r \frac{V_0}{L} - \frac{32m}{D_H^2} \right) V_0 \left(1 - \frac{x}{L} \right)$$ (7)

where: $P = P_0$ @ $x = 0$

$$P(x) = P_0 + V_0 \left(r \frac{V_0}{L} - \frac{32m}{D_H^2} \right) \left(x - \frac{x^2}{2L} \right)$$ (8)
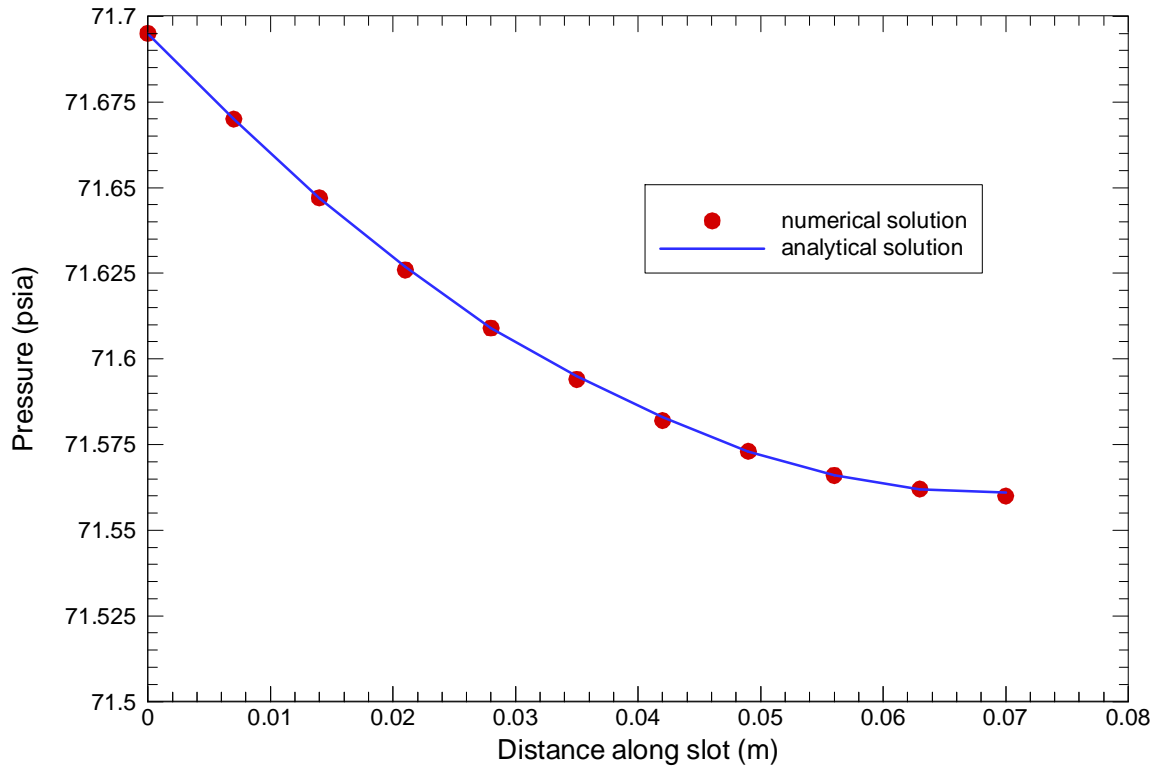
Fig. 10: Axial pressure profiles in a supply channel.

Figure 11 is a drawing of axial flow through a channel with uniform flow in through the
bottom of the channel. Equation (9) is an ordinary first-order differential equation which
governs this flow. Equation (10) is the solution to the differential equation and an
expression for the axial pressure profile in the channel. The differential equation is
derived and integrated to produce the solution in Appendix B. Figure 12 shows a
comparison between model results and the analytical solution for the axial pressure
distribution in a supply channel near the center of the flow distributor. The agreement is
very good. The assumed permeability of the porous layer in this case is low and the flow
in the bottom of the channel is therefore close to uniform axially. Again this is generally
not the case.
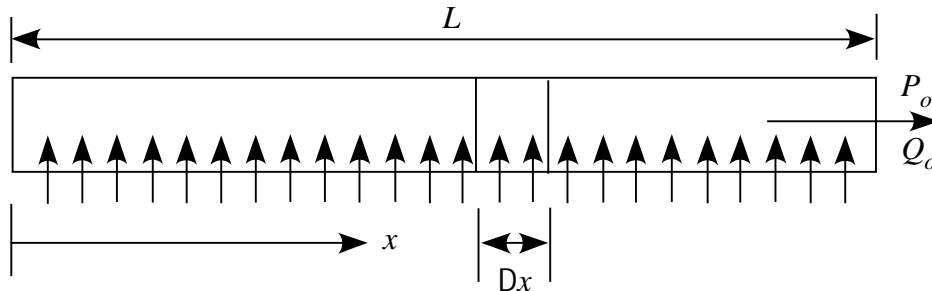
Fig.11: Schematic of axial flow through a channel with uniform flow in through the
         bottom of the channel.

Washington Savannah River Company   WSRC-STI-2006-00133
Hydrogen Electrolyzer Flow Distributor Model   Revision 0
September 2006   Page 11 of 47

$$\frac{dP}{dx} = -\left(\frac{2rV_0}{L} + \frac{32m}{D_H^2}\right)\frac{x}{L}V_0 \tag{9}$$

where: $P = P_0$ @ $x = L$

$$P(x) = P_0 + \frac{V_0}{2L}\left(\frac{2rV_0}{L} + \frac{32m}{D_H^2}\right)\left(L^2 - x^2\right) \tag{10}$$
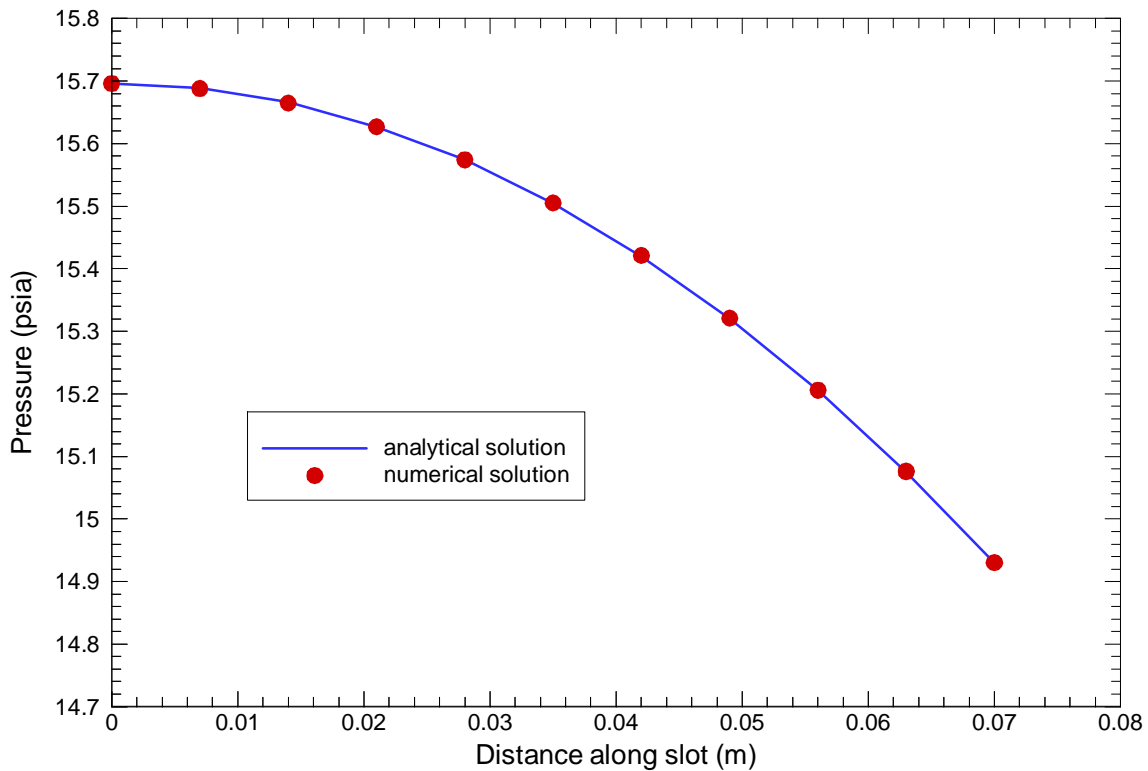
Fig. 12: Axial pressure profiles in an exhaust channel.

Results

Model predictions of steady-state flow and pressure distributions in three electrolyzer flow distributor designs are presented. The first is the current design, which is nominally 2.75 in. square and has 30 channels. The second design is also nominally 2.75 in. square, but it has 16 instead of 30 channels. The third design is nominally 5.5 in. square and has 30 channels. The channel spacing in the third design is essentially the same as that in the second design. The presented results are axial pressure profiles in adjacent supply and exhaust channels and the axial distribution of cross-flow between the two channels. The results for each flow distributor design consist of pressure and cross-flow distributions for three sets of supply and exhaust channels: the top two channels, the bottom two channels,

Washington Savannah River Company
Hydrogen Electrolyzer Flow Distributor Model
September 2006

WSRC-STI-2006-00133
Revision 0
Page 12 of 47

and a pair of channels in the middle. The top and bottom pairs of channels are different from the rest of the channels. The top channel, channel #1, is a supply channel from which the cross-flow effluent flows in a single direction, towards channel #2. The bottom channel is unique because it is an exhaust channel which receives cross-flow from a single adjacent supply channel.

Results for the extant electrolyzer flow distributor design are shown in figures 13 through 15. The anolyte is an aqueous solution of 30 weight percent sulfuric acid. The total flowrate through the flow distributor is 0.6 l/min, and the pressure drop across the flow distributor is 2.834 psi. Figure 13a shows the axial pressure profiles of the flows in the top set of adjacent supply and exhaust channels. The pressure difference between the two profiles at a specific axial location is the driving pressure for the cross-flow at that location. Figure 13b shows the normalized axial cross-flow distribution in the porous layer between the two channels. The cross-flow is normalized by the average flowrate in the porous layer. It is higher than the average cross-flow flowrate for the entire axial distance between the two channels, because all of the effluent cross-flow from channel #1 flows in the one direction. The effluent for the rest of the supply channels flows in two directions. The cross-flow flowrate varies between a minimum +4 % and a maximum of +23 % of the average flowrate.

Figure 14 shows axial pressure distributions for supply channel #15 and exhaust channel #16 and the axial distribution of the cross-flow between the two channels. Figure 14b shows the normalized axial cross-flow distribution in the porous layer between the two channels. This distribution is representative of the cross-flow in the central region of the flow distributor. The flow varies from a minimum of 5 % below the average flowrate to a maximum 10 % above the average flowrate.

Figure 15 shows axial pressure distributions for supply channel #29 and exhaust channel #30 and the axial distribution of the cross-flow between the two channels. Figure 15b shows the normalized axial cross-flow distribution in the porous layer between the two channels. It is higher than the average cross-flow flowrate for the entire axial distance between the two channels, because channel #30 receives cross-flow only from channel #29. The axial pressure distribution in channel #29 is similar to that in channel #15, and the pressures in channel #30 are lower than those in channel #16. The flowrate varies between a minimum +6 % and a maximum of +12 % of the average flowrate.

Figure 16 shows the axial distributions of cross-flow between seven sets of supply and exhaust channels in the current design electrolyzer flow distributor. The distribution of cross-flow flowrate in the cross-flow direction is fairly uniform except near the two ends. The flowrates are high between the end channels and the adjacent inboard channels, between channels #1 and 2 and between channels # 29 and 30. The flowrates between the next set of channels proceeding inward, cross-flow from channels #3 to #2 and cross-flow from channels #29 to #28, are slightly lower than the flowrate of the uniform cross-flow distribution, in the direction perpendicular to the channels, in the central portion of the porous layer.
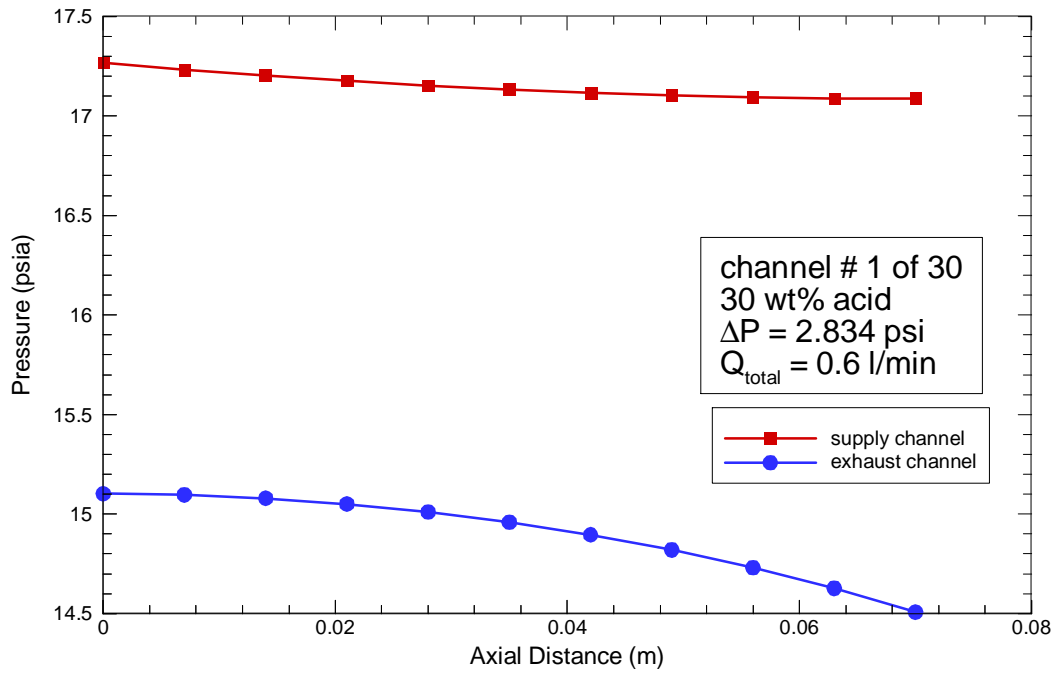
(a)
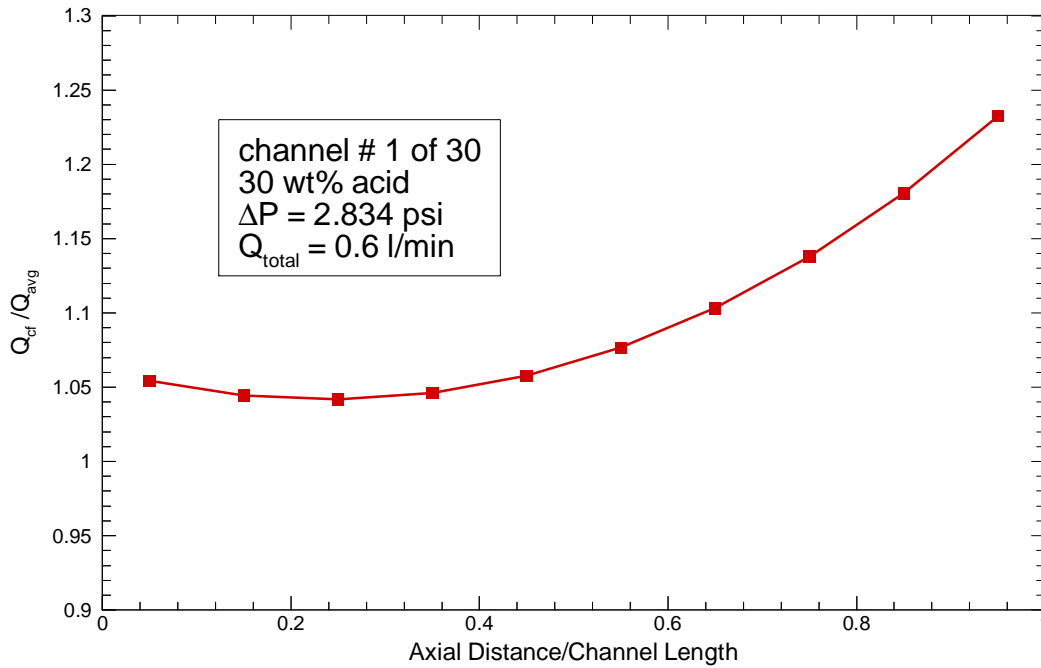
(b)

Fig. 13: Channel pressure profiles for supply channel #1 and the adjacent exhaust channel #2 for the current design flow distributor, and the axial distribution of cross-flow between the two channels.

Washington Savannah River Company   WSRC-STI-2006-00133
Hydrogen Electrolyzer Flow Distributor Model   Revision 0
September 2006   Page 14 of 47

(a)

(b)

Fig. 14: Channel pressure profiles for supply channel #15 and the adjacent exhaust channel #16 for the current design flow distributor, and the axial distribution of cross-flow between the two channels.

Washington Savannah River Company
Hydrogen Electrolyzer Flow Distributor Model
September 2006

WSRC-STI-2006-00133
Revision 0
Page 15 of 47

(a)

(b)

Fig. 15: Channel pressure profiles for supply channel #29 and the adjacent exhaust channel #30 for the current design flow distributor, and the axial distribution of cross-flow between the two channels.

Washington Savannah River Company
Hydrogen Electrolyzer Flow Distributor Model
September 2006

WSRC-STI-2006-00133
Revision 0
Page 16 of 47

Fig. 16: Axial distribution of cross-flow between several sets of supply/exhaust channels.

Figure 17 shows overall pressure drop versus flowrate for the existing 30 channel flow distributor and a similar sized 16 channel flow distributor. The channels are the same size in both designs, the only difference is the channel separation distance is doubled in the 16 channel flow distributor. For a given flowrate, the pressure drop is essentially quadrupled in the 16 channel design, which has 15 instead 29 regions between channels. For a given flowrate, the superficial velocity is almost doubled in the 16 channel design. The cross-flow pressure drop between channels is linear with distance, and for laminar flow, it is linear with superficial velocity. Doubling both the superficial velocity and flow distance quadruples the pressure drop. Local mass transfer rates in the porous media are functions of the superficial velocity, and therefore this parameter is kept constant for comparisons of the hydraulic behavior of different flow distributor designs. The average superficial velocity is 2.767×10^{-2} m/s for the 30 channel flow distributor with a flowrate of 0.6 l/min.

Washington Savannah River Company
Hydrogen Electrolyzer Flow Distributor Model
September 2006

WSRC-STI-2006-00133
Revision 0
Page 17 of 47
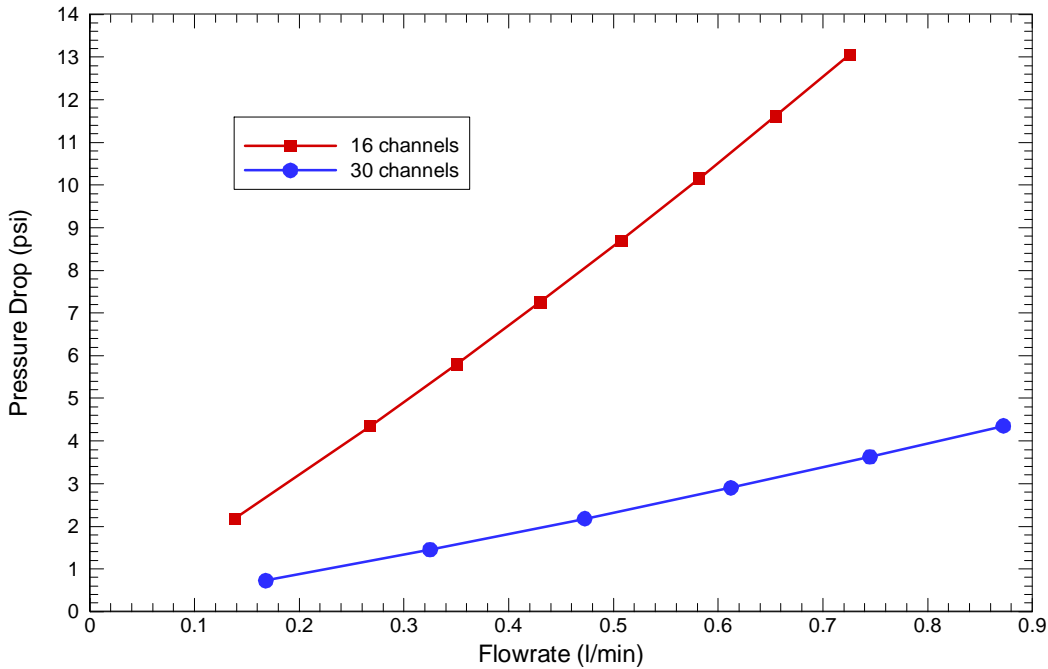
Fig. 17: Overall flow distributor pressure drop vs flowrate for the existing 30 channel
flow distributor and a similar sized 16 channel flow distributor.

Figures 18 through 20 show axial pressure profiles in three pairs of adjacent supply and
exhaust channels, and also axial distributions of the cross-flow between the channels for a
16 channel flow distributor. The anolyte is again an aqueous solution of 30 weight
percent sulfuric acid. The overall flowrate is 0.3 l/min, and the pressure drop is 4.918
psi. Figure 18 shows the results for supply channel #1 and exhaust channel #2. Again
the cross-flow is higher than the electrolyzer average value for the entire axial length of
the region between the two channels. The flowrate varies between a minimum +2 % and
a maximum of +11 % of the average flowrate. Figure 19 shows the results for supply
channel #7 and exhaust channel #8. The flowrate varies between a minimum -3 % and a
maximum of +5 % of the average flowrate, which is approximately half of the variation
for the center channels of the 30 channel design. Figure 20 shows the results for supply
channel #15 and exhaust channel #16. The flowrate varies between a minimum +3 % and
a maximum of +6 % of the average flowrate.

Washington Savannah River Company
Hydrogen Electrolyzer Flow Distributor Model
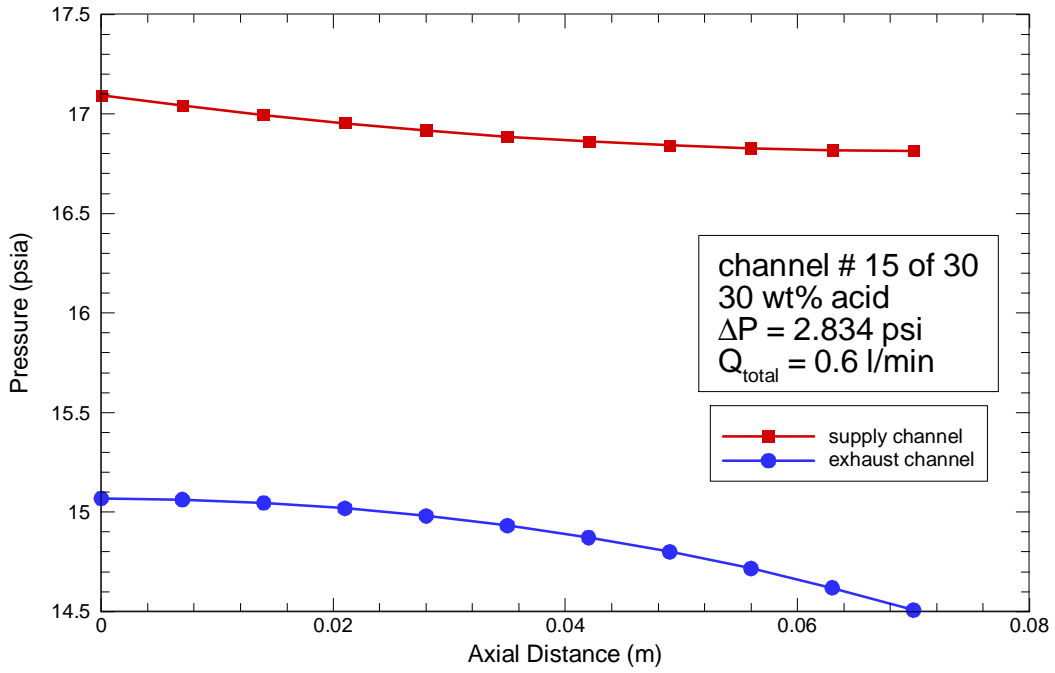September 2006

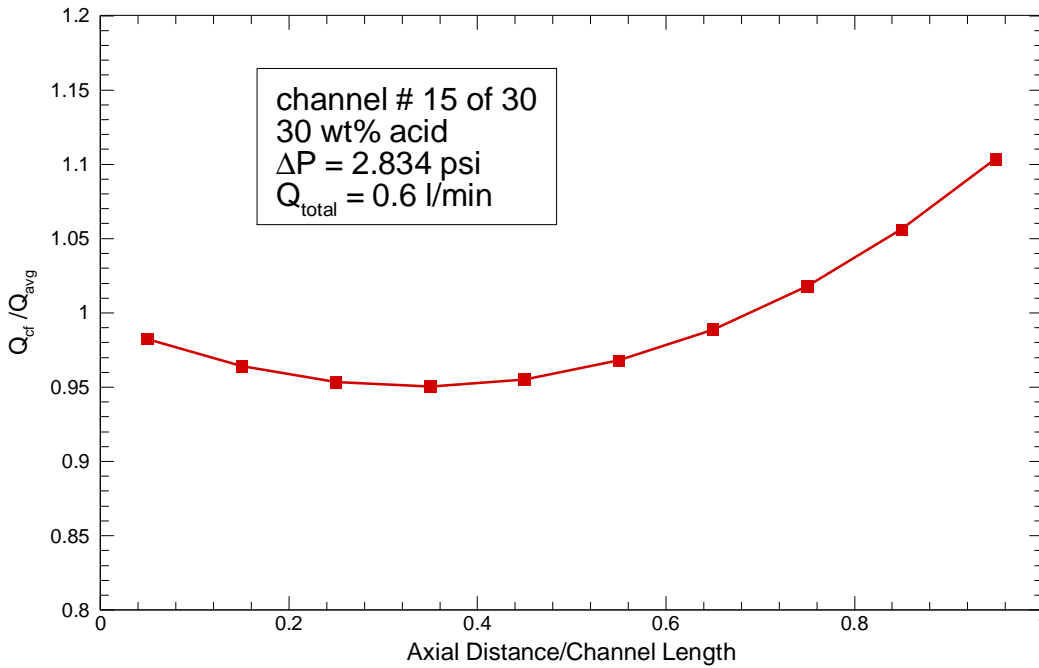WSRC-STI-2006-00133
Revision 0
Page 18 of 47
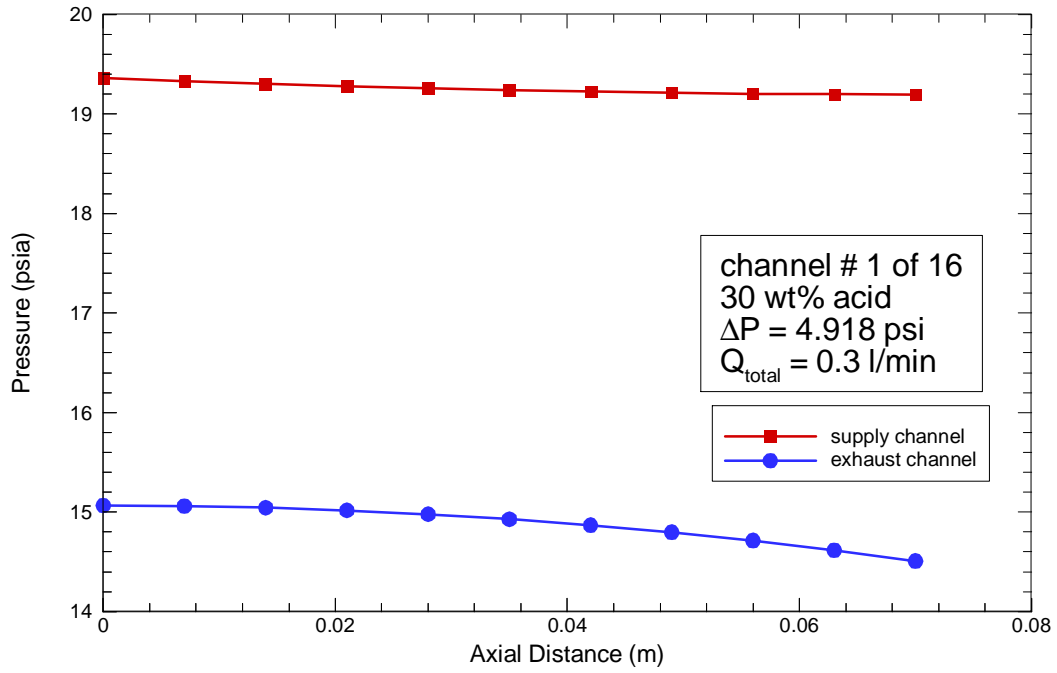
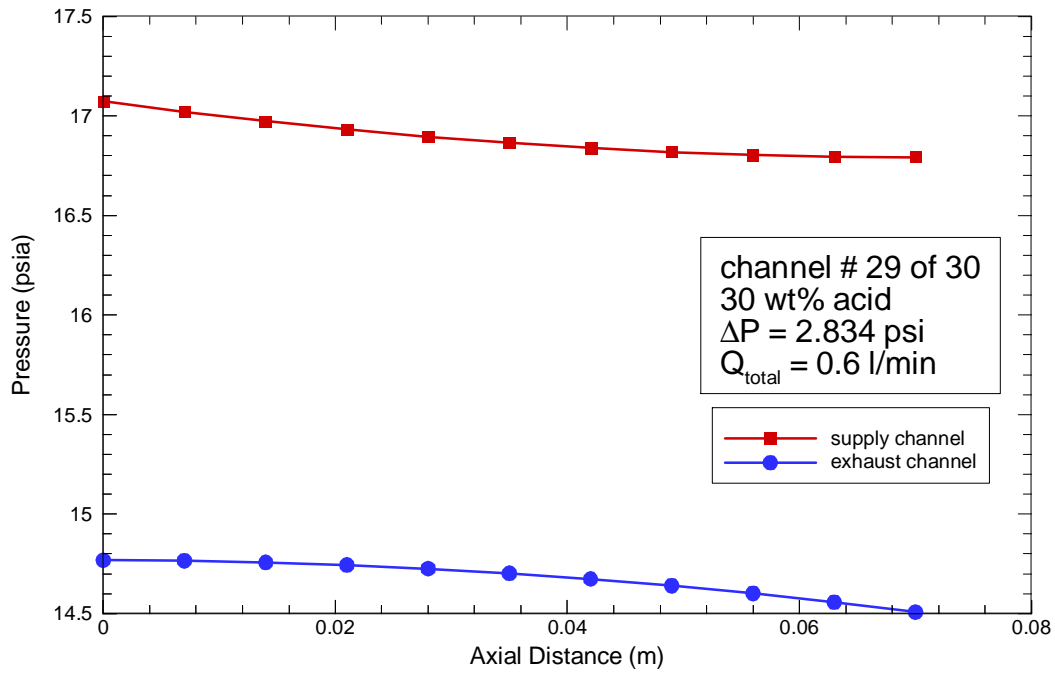(a)
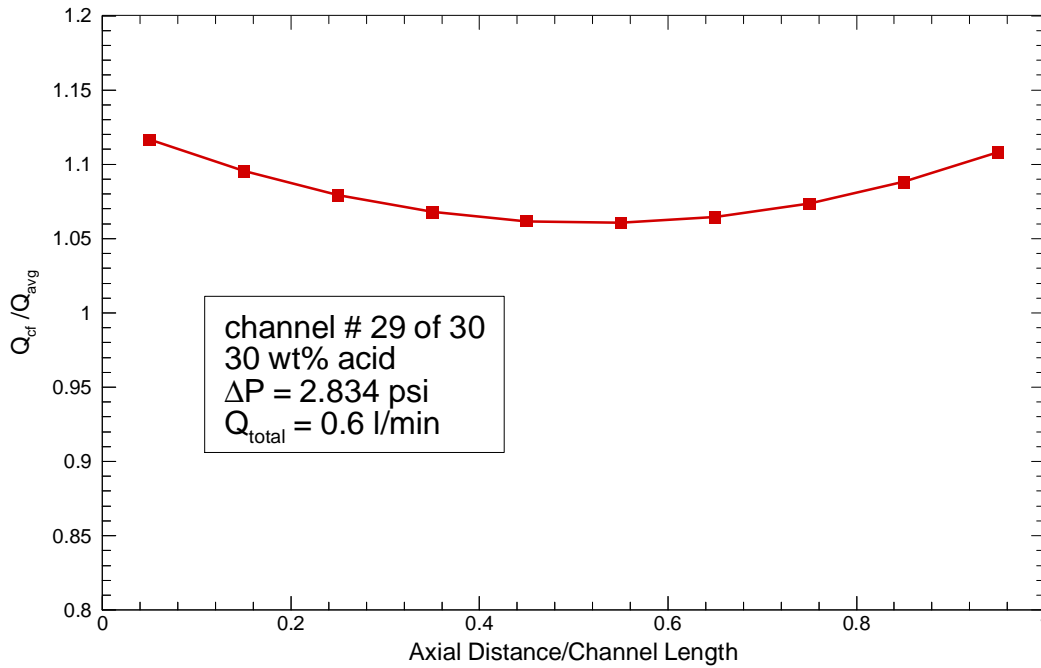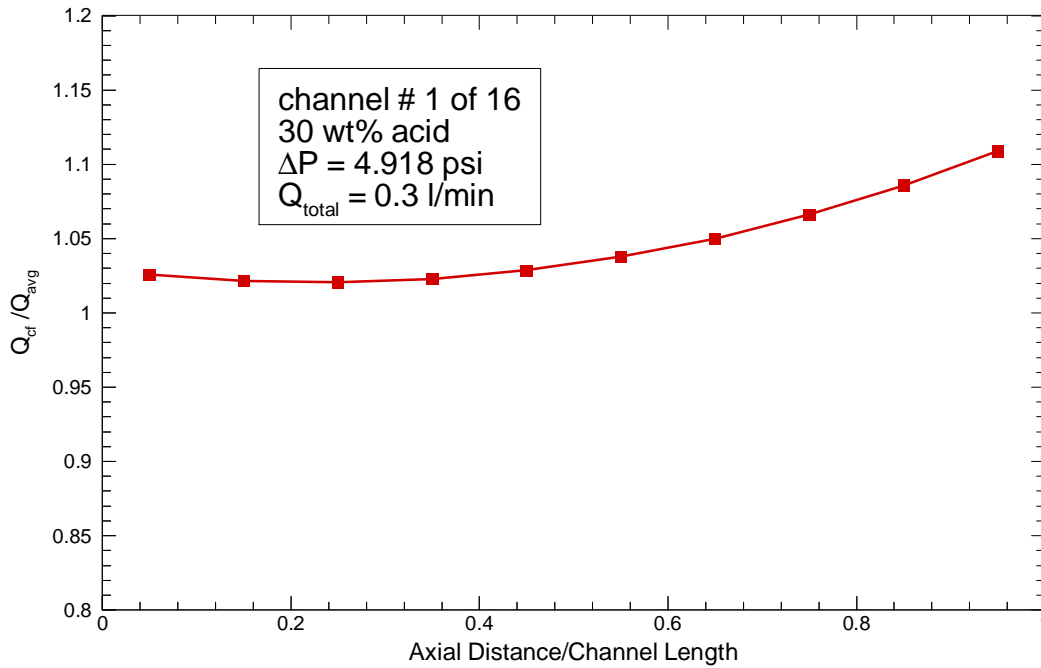

(b)

Fig. 18: Channel pressure profiles for supply channel #1 and the adjacent exhaust channel #2 for a flow distributor with 16 channels, and the axial distribution of cross-flow between the two channels.

Washington Savannah River Company   WSRC-STI-2006-00133
Hydrogen Electrolyzer Flow Distributor Model   Revision 0
September 2006   Page 19 of 47

(a)

(b)

Fig. 19: Channel pressure profiles for supply channel #7 and the adjacent exhaust channel #8 for a flow distributor with 16 channels, and the axial distribution of cross-flow between the two channels.

Washington Savannah River Company
Hydrogen Electrolyzer Flow Distributor Model
September 2006

WSRC-STI-2006-00133
Revision 0
Page 20 of 47

(a)

(b)

Fig. 20: Channel pressure profiles for supply channel #15 and the adjacent exhaust channel #16 for a flow distributor with 16 channels, and the axial distribution of cross-flow between the two channels.
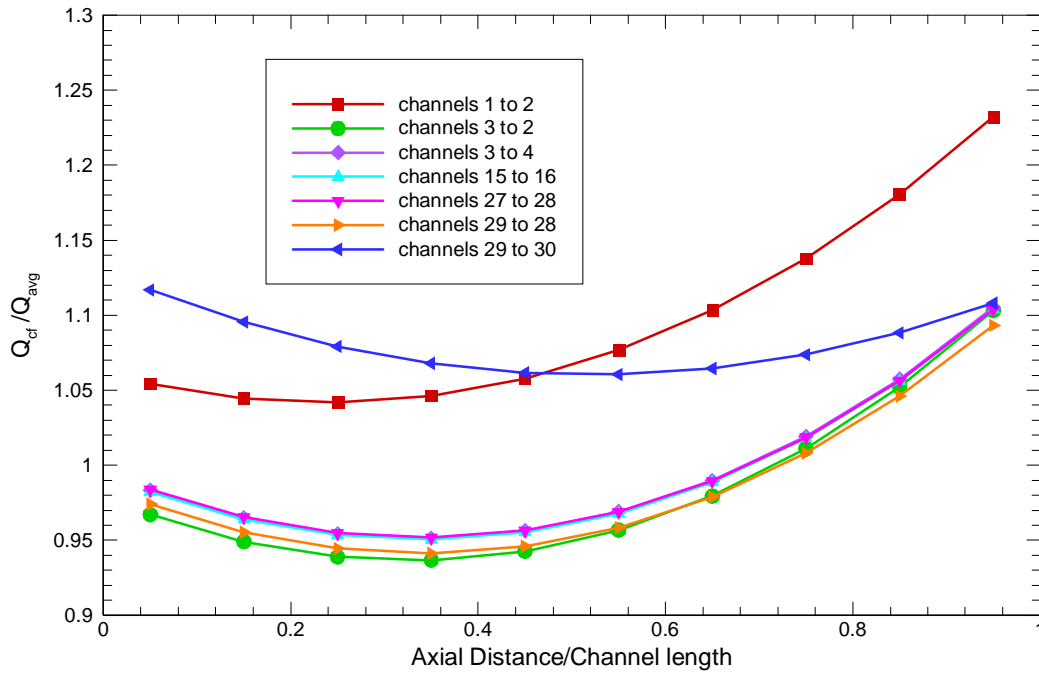
Figure 21 shows the overall pressure drop versus flowrate for the third flow distributor design. This flow distributor is 5.5 inches square rather than the 2.75 inches square of the

previous two designs. It has 30 channels with a channel spacing essentially the same as the 16 channel second design. The channel flow area is the same as in the other two designs, but the channel length is doubled.
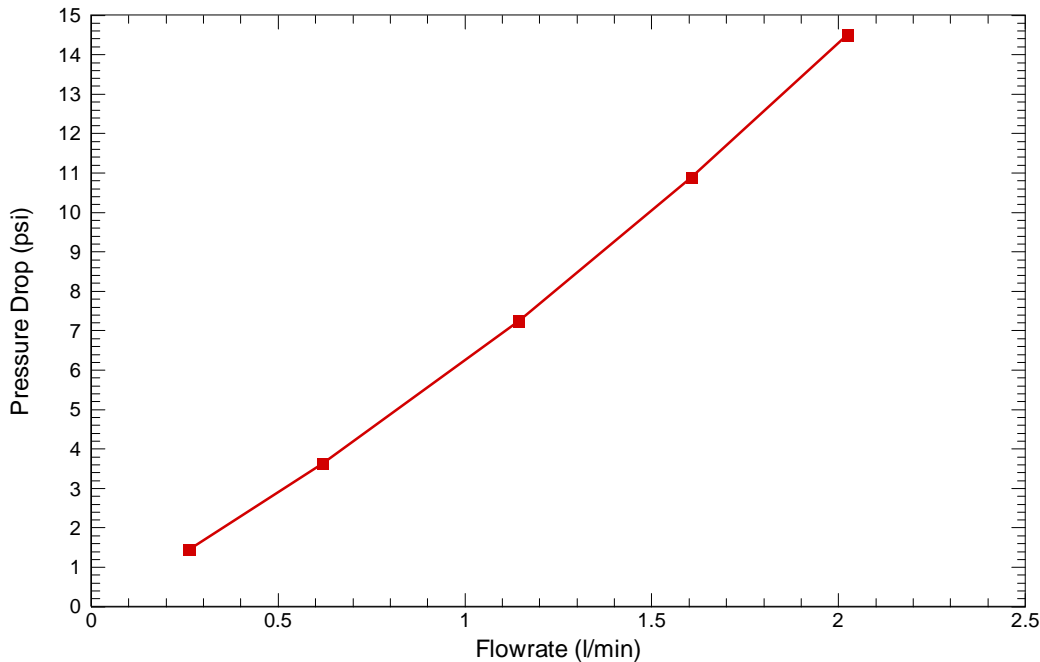
Fig. 21: Overall flow distributor pressure drop vs flowrate for a 30 channel square
          flow distributor with twice the channel length as that in the current design.

Figures 22 through 24 show axial pressure profiles in three pairs of adjacent supply and exhaust channels, and also axial distributions of the cross-flow between the channels. The anolyte is again an aqueous solution of 30 weight percent sulfuric acid. The overall flowrate is 1.2 l/min, and the pressure drop is 7.689 psi. Figure 22 shows the results for supply channel #1 and exhaust channel #2. Again the cross-flow is higher than the electrolyzer average value for the entire axial length of the region between the two channels. The flowrate varies between a minimum +6 % and a maximum of +40 % of the average flowrate. Figure 23 shows the results for supply channel #15 and exhaust channel #16. The flowrate varies between a minimum -8 % and a maximum of +19 % of the average flowrate. Figure 24 shows the results for supply channel #29 and exhaust channel #30. The flowrate varies between a minimum +9 % and a maximum of +20 % of the average flowrate. The cross-flow is considerably less uniform than in the second design with 16 channels. The difference is due to the longer channel lengths in the third design. The axial pressure drops in the central supply and exhaust channels of the larger flow distributor are respectively 1.05 and 2.2 psi. In the smaller 16 channel flow distributor, the axial pressure drops in the central supply and exhaust channels are respectively 0.3 and 1.0 psi.
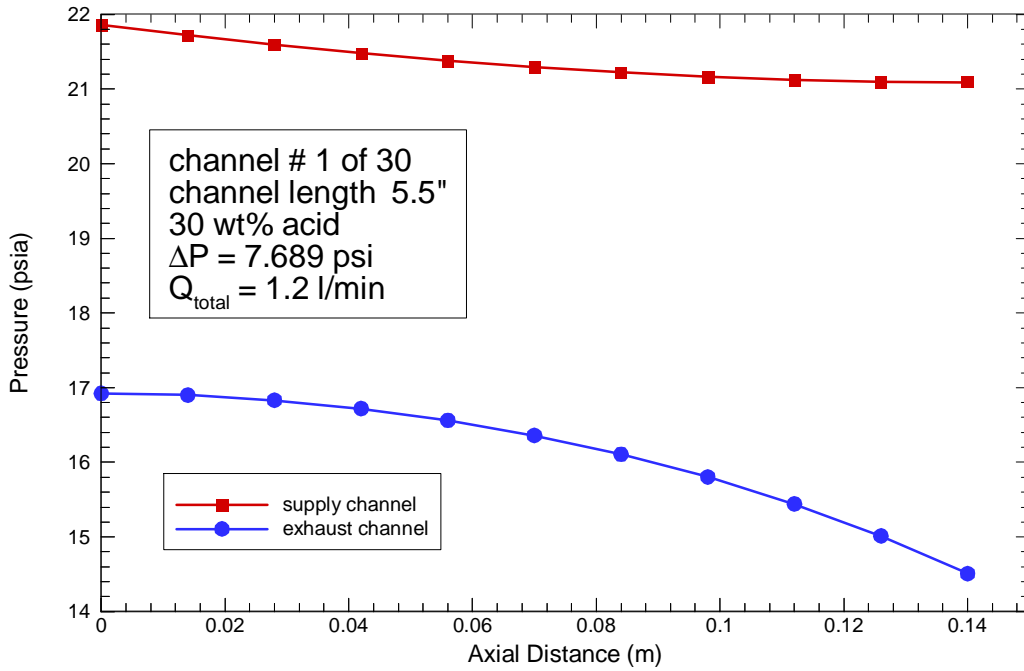
(a)
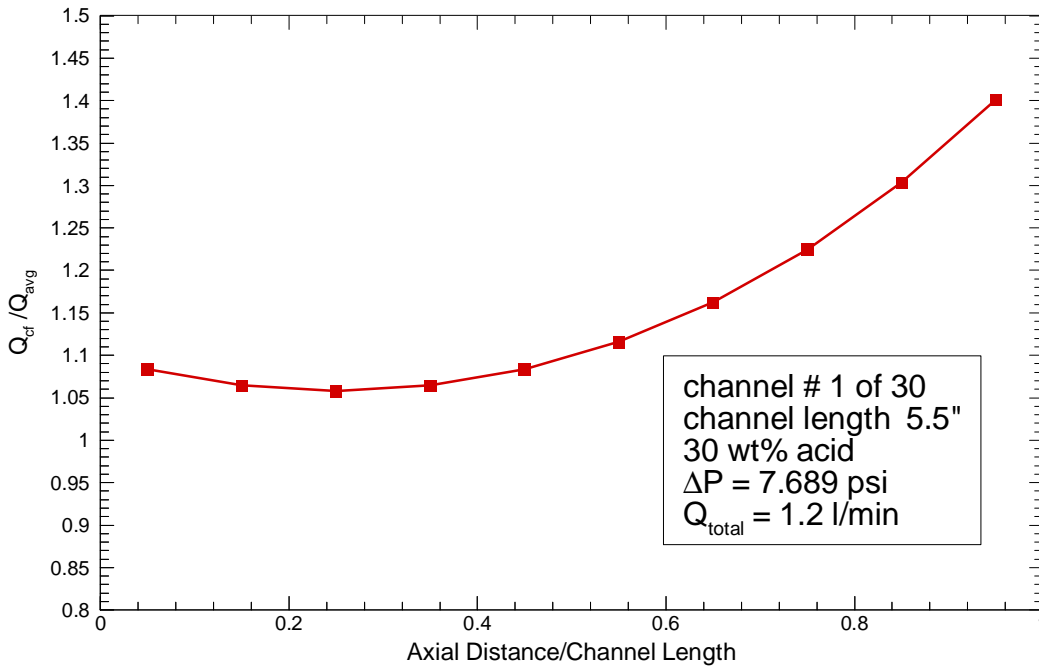
(b)

Fig. 22: Channel pressure profiles for supply channel #1 and the adjacent exhaust
　　　　channel #2 for a 5.5 inch square flow distributor with 30 channels, and the axial
　　　　distribution of cross-flow between the two channels.

Washington Savannah River Company
Hydrogen Electrolyzer Flow Distributor Model
September 2006

WSRC-STI-2006-00133
Revision 0
Page 23 of 47

(a)

channel # 15 of 30
channel length 5.5"
30 wt% acid
ΔP = 7.689 psi
Q_{total} = 1.2 l/min

(b)

channel # 15 of 30
channel length 5.5"
30 wt% acid
ΔP = 7.689 psi
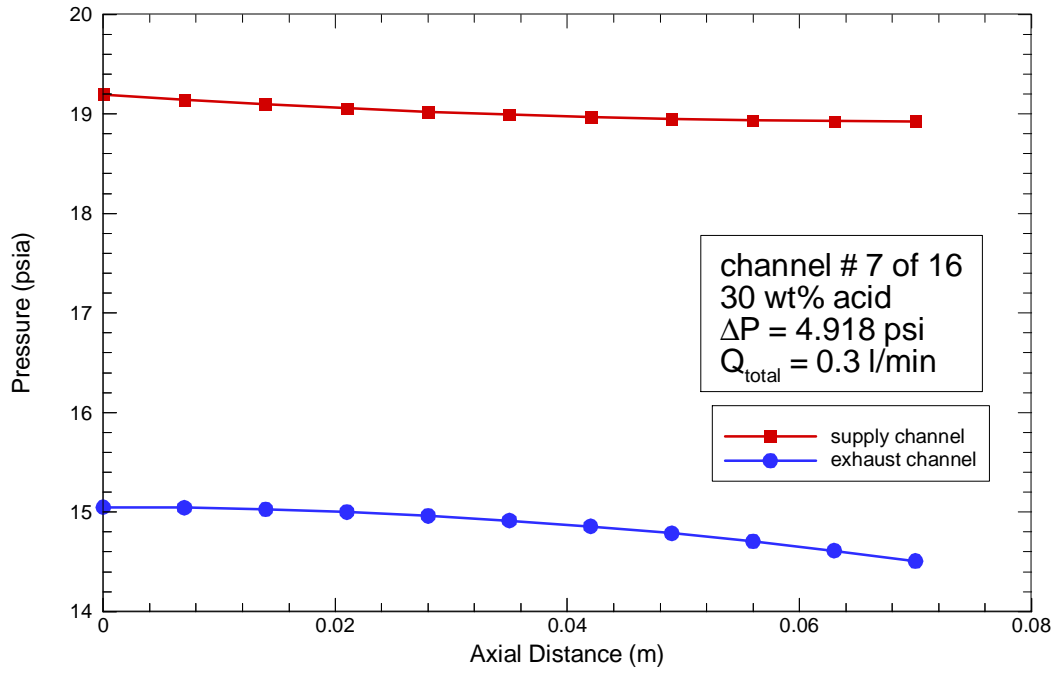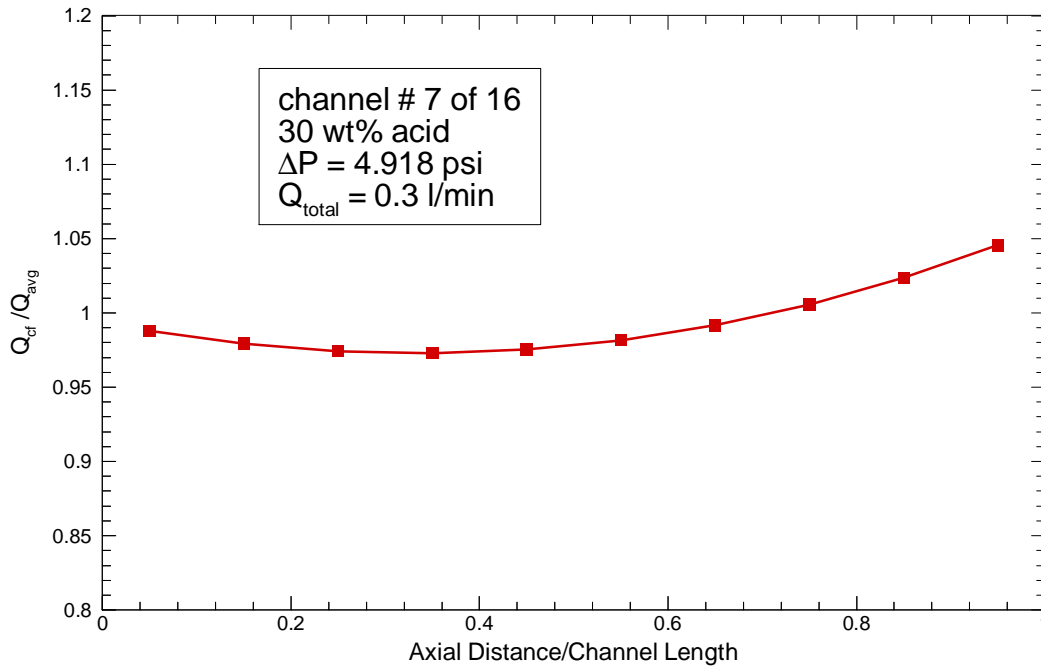Q_{total} = 1.2 l/min

Fig. 23: Channel pressure profiles for supply channel #15 and the adjacent exhaust channel #16 for a 5.5 inch square flow distributor with 30 channels, and the axial distribution of cross-flow between the two channels.

Washington Savannah River Company
Hydrogen Electrolyzer Flow Distributor Model
September 2006

WSRC-STI-2006-00133
Revision 0
Page 24 of 47

(a)

(b)

Fig. 24: Channel pressure profiles for supply channel #29 and the adjacent exhaust channel #30 for a 5.5 inch square flow distributor with 30 channels, and the axial distribution of cross-flow between the two channels.
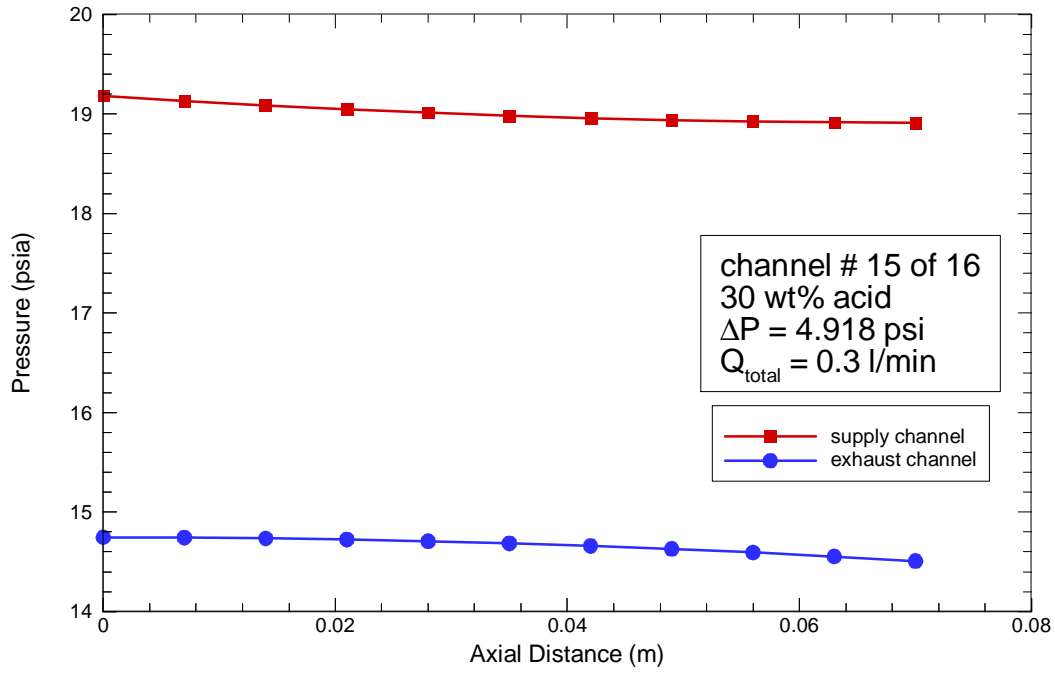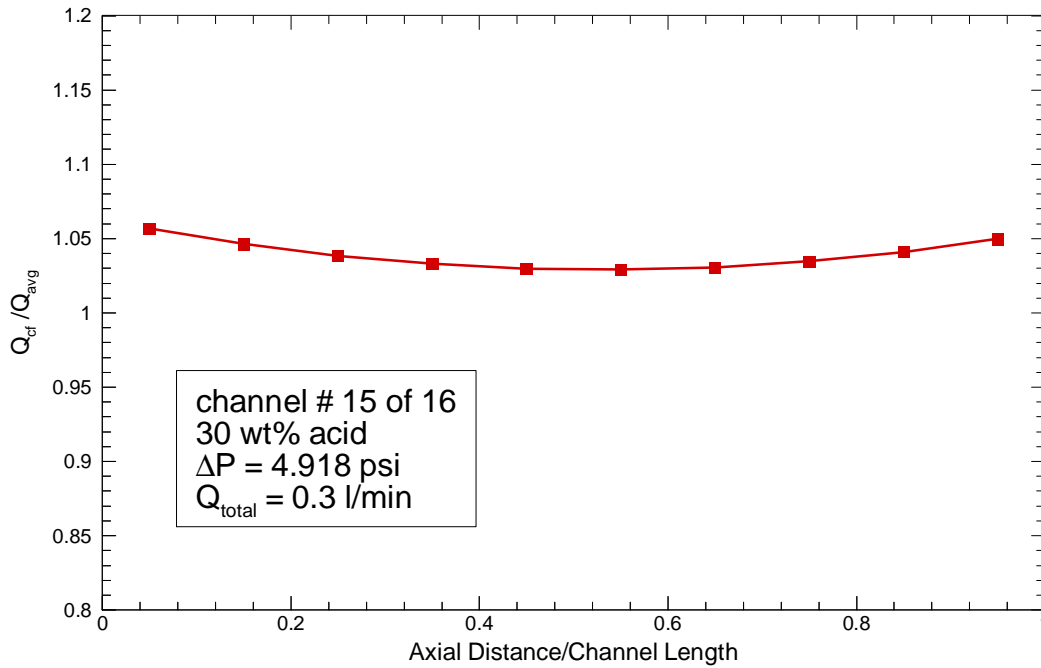
Figure 25 shows axial pressure profiles of supply channel #15 and exhaust channel #16 and the axial distribution of cross-flow between the two channels for the larger flow

Washington Savannah River Company   WSRC-STI-2006-00133
Hydrogen Electrolyzer Flow Distributor Model   Revision 0
September 2006   Page 25 of 47

distributor design with a reduced flowrate. The overall pressure drop is 1.0 psi and the flowrate is 0.18 l/min. This flowrate is 15 % of the case with results shown in figure 23. The cross-flow flowrate varies between a minimum of -6 % and a maximum of +9 % of the average flowrate. This variation is a little over half of the variation at an electrolyzer flowrate of 1.2 l/min.

Figure 26 shows axial pressure profiles of supply channel #15 and exhaust channel #16 and the axial distribution of cross-flow between the two channels for the larger flow distributor design with the channel cross-sectional flow area doubled. The channel spacing remains the same. The overall pressure drop is 5.288 psi and the flowrate is 1.2 l/min., the same flowrate as for the results in figures 22 through 24. The cross-flow flowrate varies between a minimum -2 % and a maximum of +7 % of the average flowrate. This is approximately a quarter of the variation shown in figure 23 for the case with smaller cross-section area channels.

Washington Savannah River Company
Hydrogen Electrolyzer Flow Distributor Model
September 2006

WSRC-STI-2006-00133
Revision 0
Page 26 of 47

(a)
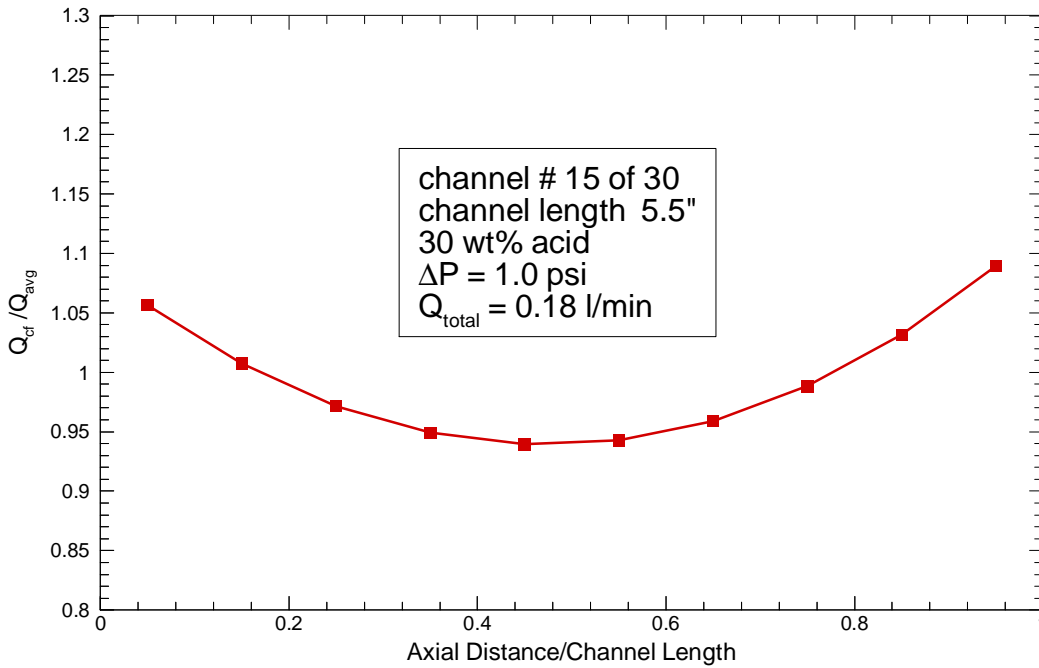
(b)

Fig. 25: Channel pressure profiles for supply channel #15 and the adjacent exhaust channel #16 for a 5.5 inch square flow distributor with 30 channels, and the axial distribution of cross-flow between the two channels.
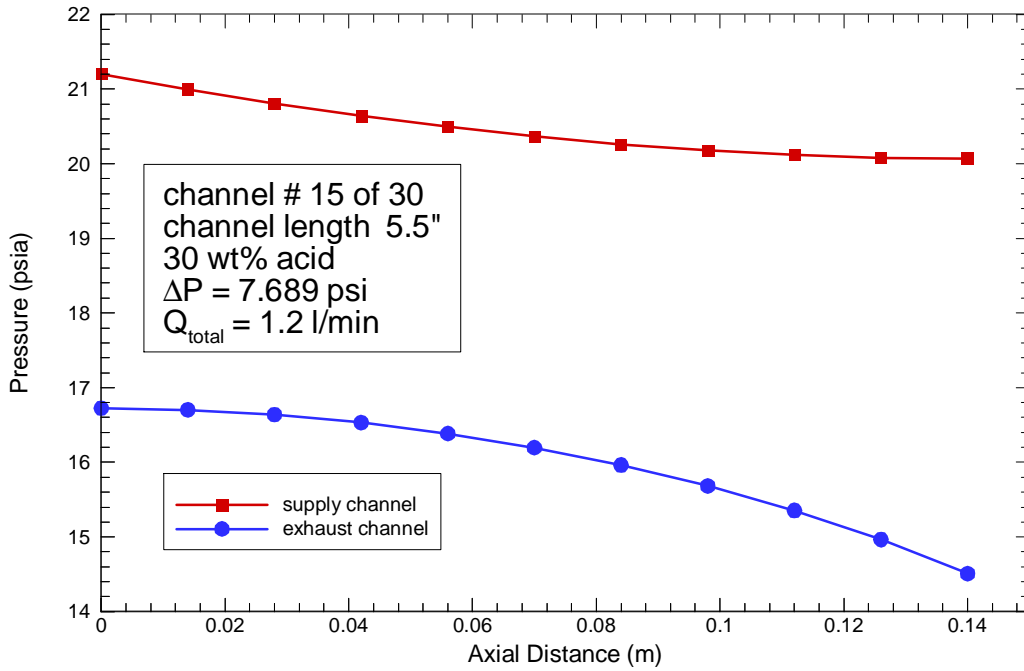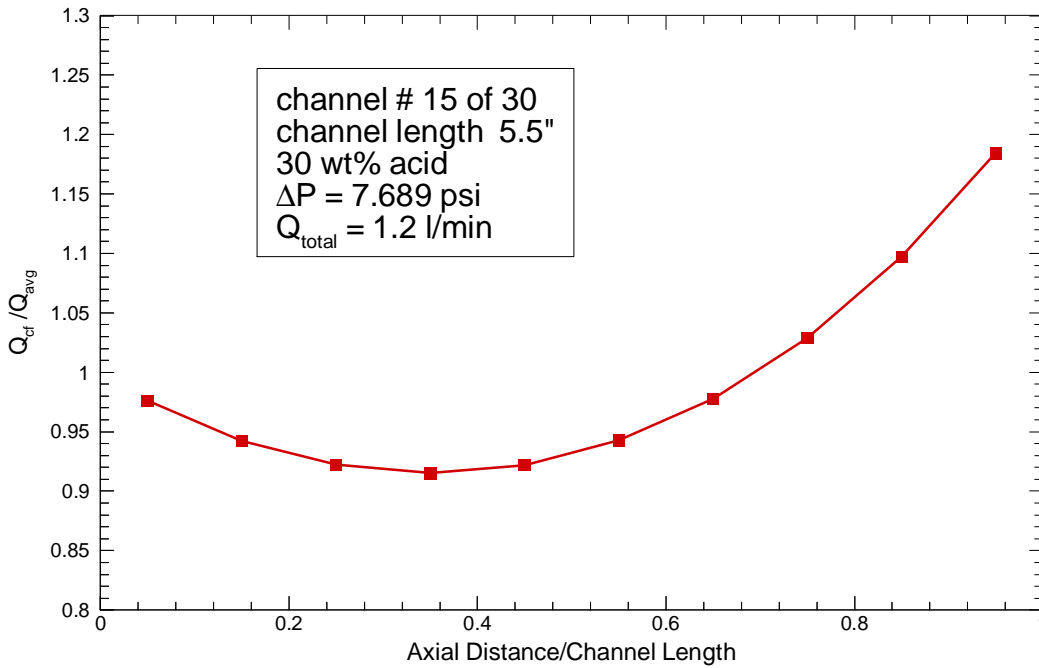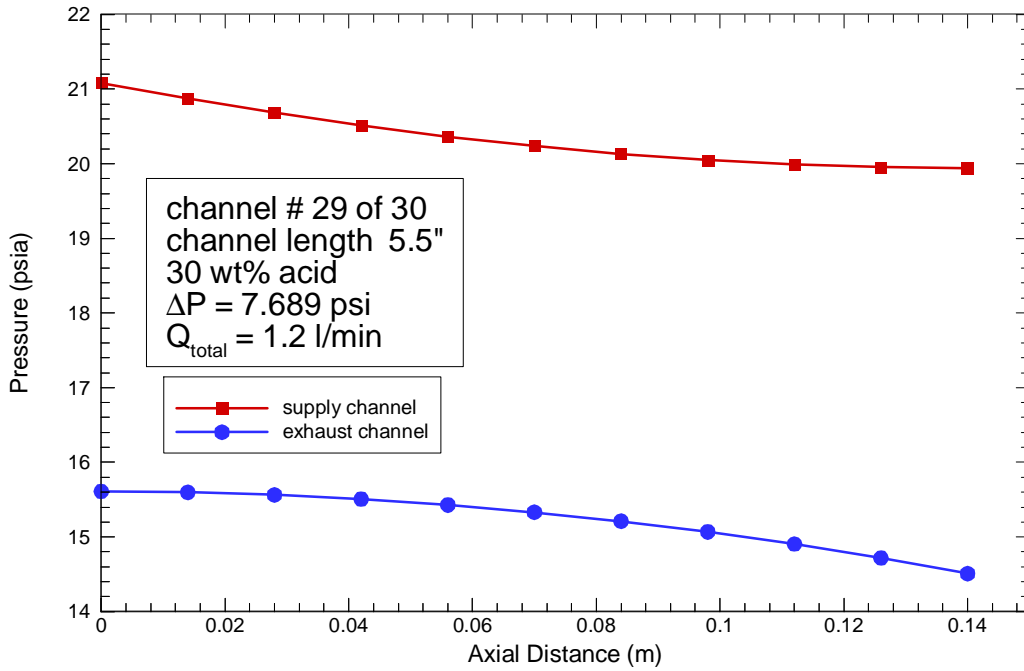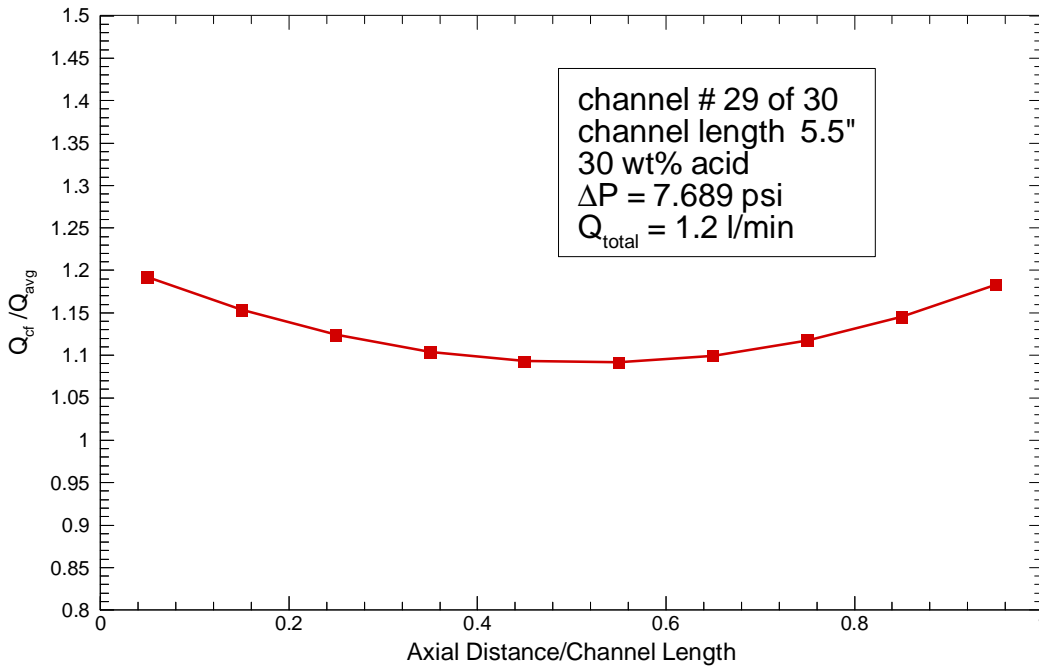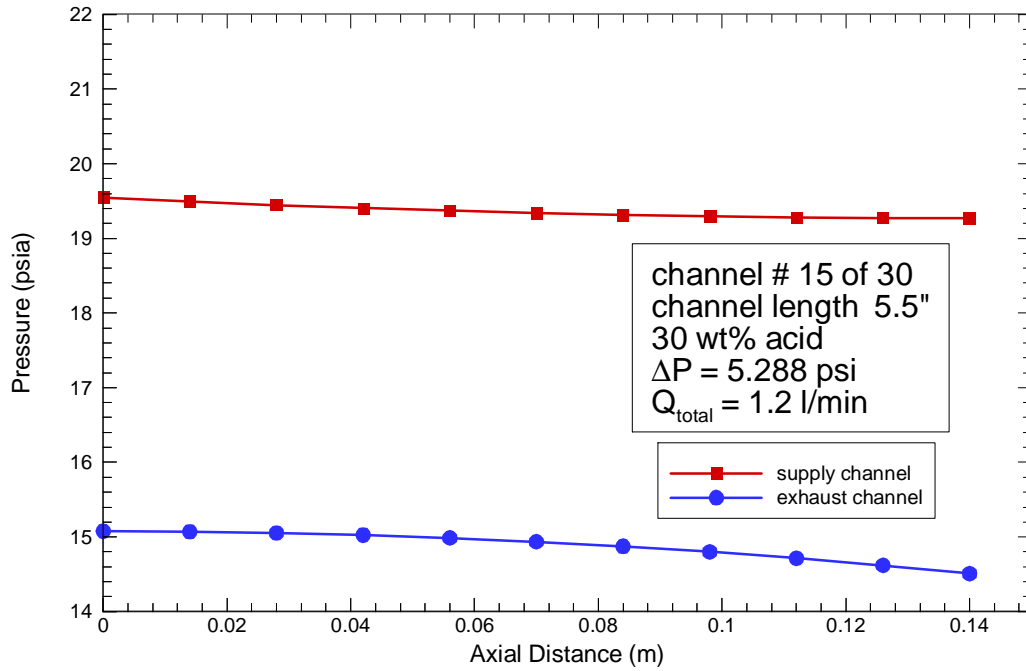
(a)
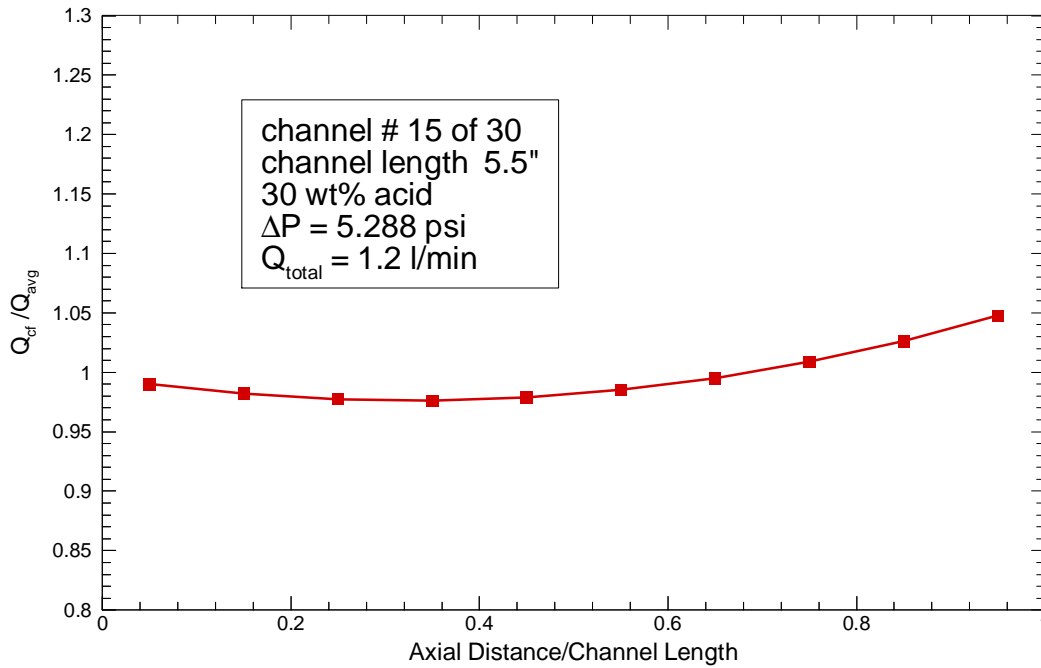
(b)

Fig. 26: Channel pressure profiles for supply channel #15 and the adjacent exhaust
          channel #16 for a 5.5 inch square flow distributor with 30 channels, and the axial
          distribution of cross-flow between the two channels. The channel flow areas
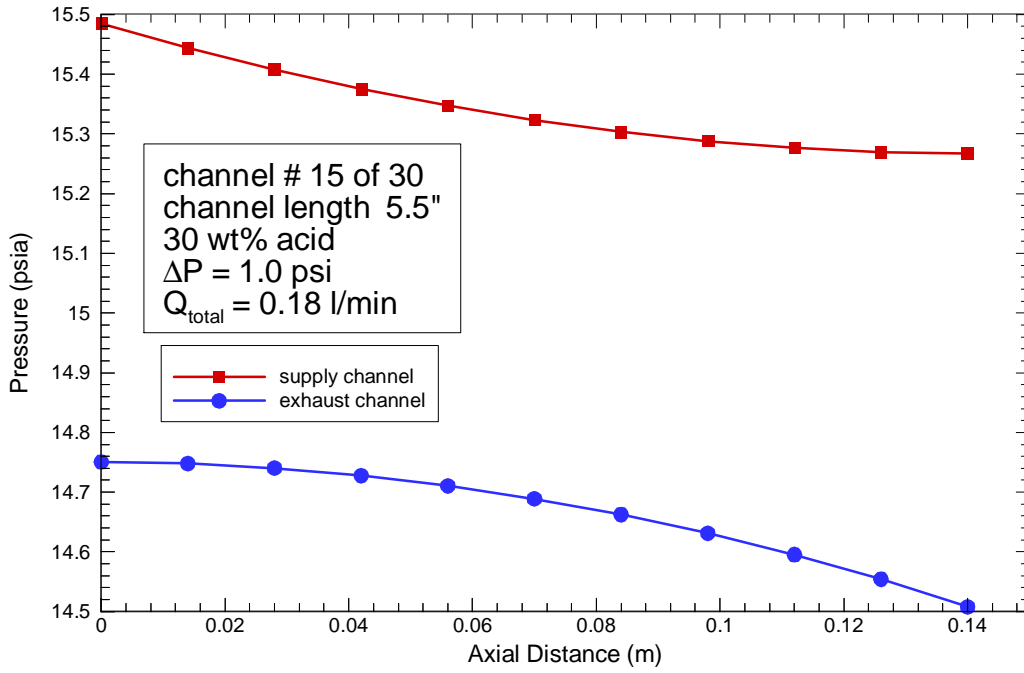   have been doubled.

Washington Savannah River Company   WSRC-STI-2006-00133
Hydrogen Electrolyzer Flow Distributor Model   Revision 0
September 2006   Page 28 of 47

Conclusions

A steady-state numerical hydraulics model of the electrolyzer flow distributor has been developed. This model predicts pressure and flow distributions within the porous graphite layer on the anode side. Figure 8 shows that the model reasonably predicts pressure drop versus flowrate relationship, once the permeability of the porous layer is determined. The model correctly accounts for the viscosity effect. While the predicted internal pressure and flow distributions within the electrolyzer cannot be directly validated because of a lack of data, the good correlation between overall hydraulic behavior and data and the fact that the permeability required to achieve this fit is within the range of independently measured values, certainly supports the creditability of these results. This model will be a valuable asset in designing the next generation flow distributor.

Recommendations

Uniform flow of anolyte through the porous carbon layer adjacent to the PEM is necessary for optimum performance of an electrolyzer, but it is hardly sufficient. Mass transfer through the anolyte to the PEM surface is very important, and this aspect of the electrolyzer performance should also be modelled. Optimization of mass transfer impacts electrolyzer design parameters such as flowrate and carbon layer thickness, and these parameters in turn influence the flow distributor design. A coupled hydraulic/mass transfer model should be developed. Such a tool will be a valuable design aid.

References

1.   Bird, R. B., Stewart, W. E., Lightfoot, E. N., "Transport Phenomena", John Wiley & Sons, Inc., 1960.

2.   Feser, A., Prasad, A., Advani, S., "A Radial Flow Characterization Technique to Measure In Plane Permeability of Gas Diffusion Layers", University of Delaware, http://www.me.udel.edu/research_groups/prasad/proj/permeability.html.

Washington Savannah River Company
Hydrogen Electrolyzer Flow Distributor Model
September 2006

WSRC-STI-2006-00133
Revision 0
Page 29 of 47

Nomenclature

A	Area	$\dot{m}_{cf}$	Cross-flow mass flowrate
A_{slt}	Channel cross-sectional area	P	Pressure
D_H	Channel hydraulic diameter	Q	Volume flowrate
D_p	Porous media particle diameter	QL	Cross-flow volume flowrate
F_f	Wall friction force	Re	Reynolds number
f	Darcy friction factor	V	Velocity
K	Form loss coefficient	e	Porosity
k	Permeability	m	Viscosity
L	Length	r	Density
$\dot{m}$	Mass flowrate		

Washington Savannah River Company   WSRC-STI-2006-00133
Hydrogen Electrolyzer Flow Distributor Model   Revision 0
September 2006   Page 30 of 47

This Page Deliberately Left Blank

Washington Savannah River Company

Hydrogen Electrolyzer Flow Distributor Model

September 2006

WSRC-STI-2006-00133

Revision 0

Page 31 of 47

Appendix A   Model Equations

There are three types of momentum equations in the model: flow in the supply channels, flow in the exhaust channels, and cross-flow between the channels. The forms of the momentum equations used in the model are derived in this appendix. The recursive governing equations for the model developmental flow distributor network shown in figure 4 are also herein listed. The structure of the model allows the number of channels in the flow distributor to be easily varied.

Figure a1 is a schematic of a single control volume in a supply channel. The flow is assumed to be steady and laminar, and there is axially uniform flow out of the bottom of the control volume. Axial momentum is convected out of the control volume by this flow. Equation (a1) is the general form of the linear momentum equation. Equation (a2) is the simplified form for steady-flow. The external forces applied to the control are the pressure forces and wall friction. Due to the small channel hydraulic diameter and the high viscosity of the fluid, the channel flow is laminar, and this simplification is exploited in the formulation of the wall friction force term, equation (a5). Equation (a6) is the form of the supply channel momentum equation utilized in the model.
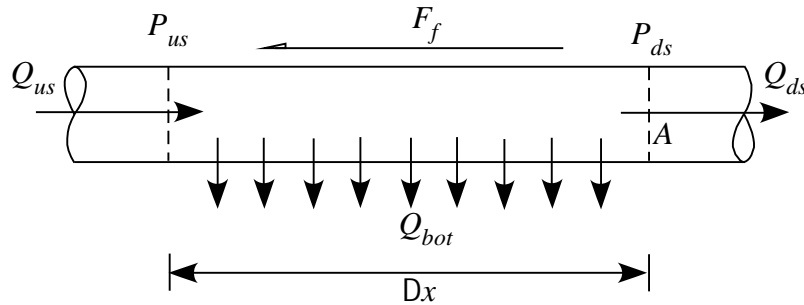
Fig. a1: Schematic of a single control volume in a supply channel.

$$\frac{d}{dt}\int_{\forall_{CV}} r \vec{V} d\forall + \oint_{A_{CV}} r \vec{V}(\vec{V}_r \cdot \hat{n}) dA = \sum \vec{F} \tag{a1}$$

$$\left(\dot{m}\vec{V}\right)_{out} - \left(\dot{m}\vec{V}\right)_{in} = \sum \vec{F} \tag{a2}$$

$$r Q_{ds}\frac{Q_{ds}}{A} + r Q_{bot}\overline{V} - r Q_{us}\frac{Q_{us}}{A} = \left(P_{us} - P_{ds}\right)A + F_f \tag{a3}$$

$$F_f = -r\frac{f\Delta x}{D_H}\frac{\overline{V}^2}{2}A \qquad \text{where:} \quad \overline{V} = \frac{1}{2A}\left(Q_{us} + Q_{ds}\right) \tag{a4}$$

$$f = \frac{64}{\mathrm{Re}_{D_H}} = \frac{64m}{r\overline{V}D_H} \qquad \text{and} \qquad F_f = -\frac{16m\Delta x}{D_H^2}\left(Q_{us} + Q_{ds}\right) \tag{a5}$$

$$Q_{ds}^2 + \frac{Q_{bot}}{2}(Q_{us} + Q_{ds}) - Q_{us}^2 = (P_{us} - P_{ds})\frac{A^2}{r} - \frac{16m\Delta xA}{rD_H^2}(Q_{us} + Q_{ds}) \tag{a6}$$

Figure a2 is a schematic of a single control volume in an exhaust channel. In this case there is axially uniform flow into the control volume. The upward flow into the channel enters the control with no axial momentum. The linear momentum equation is again applied to this flow. The flow is also laminar. Equation (a7) is the momentum equation for a control volume in the exhaust channel, and equation (a8) is the form utilized in the model.
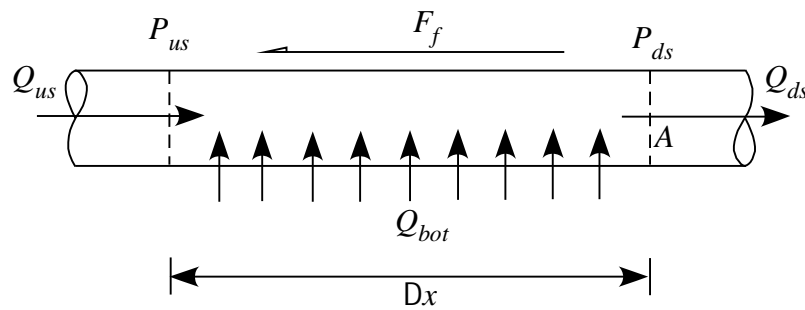
Fig. a2: Schematic of a single control volume in an exhaust channel.

$$\frac{r}{A}Q_{ds}^2 - \frac{r}{A}Q_{us}^2 = (P_{us} - P_{ds})\frac{A^2}{r} - \frac{16m\Delta xA}{rD_H^2}(Q_{us} + Q_{ds}) \tag{a7}$$

$$Q_{ds}^2 - Q_{us}^2 = (P_{us} - P_{ds})\frac{A^2}{r} - \frac{16m\Delta xA}{rD_H^2}(Q_{us} + Q_{ds}) \tag{a8}$$

The cross-flow through the porous carbon paper is assumed to be governed by the Ergun equation [x]. Figure a3 is a schematic of a control volume in the porous carbon paper. Equation (a9) is the Ergun equation for this control volume. It is expressed in terms of the superficial velocity, equation (a10). Equation (a11) is the Ergun equation in terms of the volume flowrate. The Ergun equation is applicable for porosities less than or equal to 0.5. The interstial porosity of carbon paper is at the upper end of or slightly above this range. The channel pressures drive the cross-flow, and they are defined at the corners of the control volume shown in figure a3. Equation (a12) is the Ergun equation in terms of the corner pressures. This is the form of the equation used in the model.

Washington Savannah River Company
Hydrogen Electrolyzer Flow Distributor Model
September 2006

WSRC-STI-2006-00133
Revision 0
Page 33 of 47
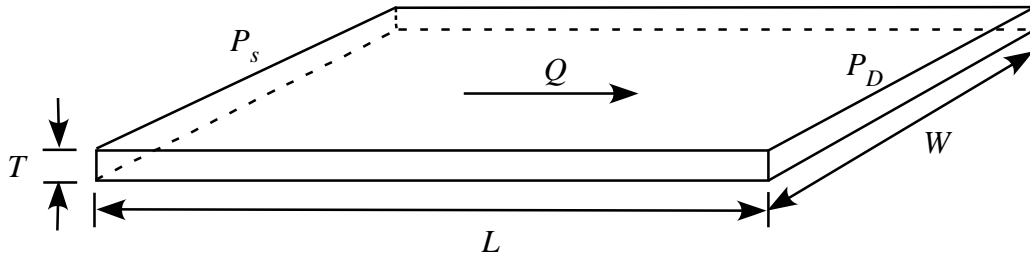
Fig. a3: Schematic of a single control volume in the porous carbon paper.

$$\frac{P_S - P_D}{L} = \frac{150 \mathrm{m} v_0}{D_p^2} \frac{(1-\mathrm{e})^2}{\mathrm{e}^3} + \frac{1.75 \mathrm{r} v_0^2}{D_p} \frac{1-\mathrm{e}}{\mathrm{e}^3} \tag{a9}$$

$$v_0 = \frac{Q}{A} = \frac{Q}{WT} \tag{a10}$$

$$\frac{P_S - P_D}{L} = \frac{150 \mathrm{m} Q}{A D_p^2} \frac{(1-\mathrm{e})^2}{\mathrm{e}^3} + \frac{1.75 \mathrm{r} Q^2}{A^2 D_p} \frac{1-\mathrm{e}}{\mathrm{e}^3} \tag{a11}$$

$$\left(P_{S_i} + P_{S_{i+1}}\right) - \left(P_{D_i} + P_{D_{i+1}}\right) = \frac{300 \mathrm{m} L}{A D_p^2} \frac{(1-\mathrm{e})^2}{\mathrm{e}^3} Q + \frac{3.5 \mathrm{r} L}{A^2 D_p} \frac{1-\mathrm{e}}{\mathrm{e}^3} Q^2 \tag{a12}$$

There is an inconsistency between the linear momentum equations used to model the channel flows and the Ergun equation used for the porous layer cross-flow. The flow into the porous layer from the supply channel has axial momentum. This component of momentum is ignored in the porous media cross-flow. The assumption of one-dimensional flow in the porous layer is reasonable and it considerably simplifies the model.

Figure a4 is a schematic of the reduced scale flow distributor network which was used to develop the model. There are five supply channels and five exhaust channels. Each channel is divided into five axial control volumes. Figure a4 also shows the flow pattern in the network. A listing of the governing equations for this network follows. There is a momentum equation and a continuity equation for each of the channel control volumes, and there is an Ergun equation for each of the cross-flow control volumes. Nine sets of equations are listed: entrance middle and exit equations for the top and bottom channels and entrance middle and exit equations for the center channels. A figure of the local sub-network precedes each set of equations.

Washington Savannah River Company   WSRC-STI-2006-00133
Hydrogen Electrolyzer Flow Distributor Model   Revision 0
September 2006   Page 34 of 47
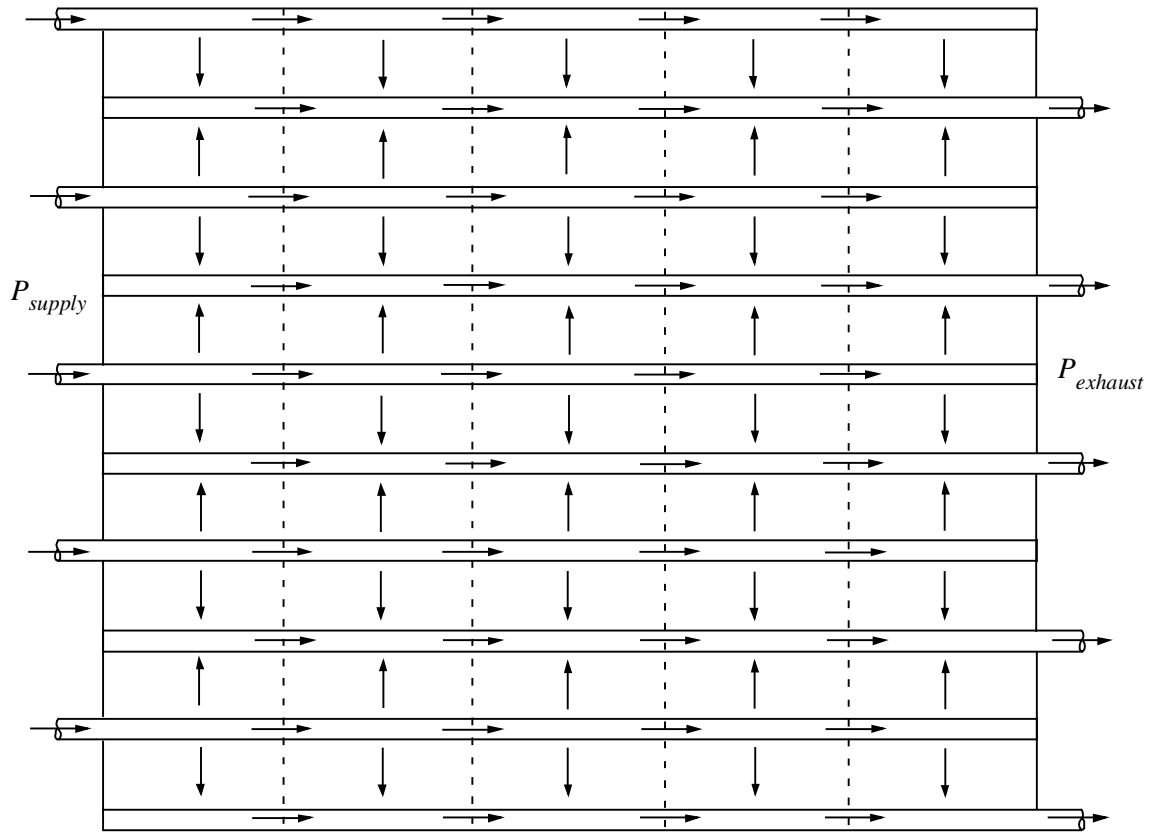
Fig. a4: Schematic of the reduced scale flow distributor used for model development.

Washington Savannah River Company
Hydrogen Electrolyzer Flow Distributor Model
September 2006

WSRC-STI-2006-00133
Revision 0
Page 35 of 47

Fig. a5: Top row entrance sub-network.

$$P_{in} = P_{1,1} + \frac{\mathrm{r}}{2A_{slt}^2}\left(1 + K_{ent}\right)Q_{1,1}^2$$

$$Q_{2,1}^2 - Q_{1,1}^2 + \tfrac{1}{2}QL_{1,1}\left(Q_{1,1} + Q_{2,1}\right) = \left(P_{1,1} - P_{2,1}\right)\frac{A_{slt}^2}{\mathrm{r}} - \frac{16\mathrm{m}\Delta x}{\mathrm{r}D_H^2}\left(Q_{1,1} + Q_{2,1}\right)$$

$$Q_{1,1} = Q_{2,1} + QL_{1,1}$$

$$Q_{2,2}^2 = \left(P_{1,2} - P_{2,2}\right)\frac{A_{slt}^2}{\mathrm{r}} - \frac{16\mathrm{m}\Delta x}{\mathrm{r}D_H^2}Q_{2,2}$$

$$QL_{1,1} + QL_{1,2} = Q_{2,2}$$

$$\left(P_{1,1} + P_{2,1}\right) - \left(P_{1,2} + P_{2,2}\right) = \frac{300\mathrm{m}\Delta z}{AD_p^2}\frac{\left(1 - \mathrm{e}\right)^2}{\mathrm{e}^3}QL_{1,1} + \frac{3.5\mathrm{r}\Delta z}{A^2 D_p}\frac{1 - \mathrm{e}}{\mathrm{e}^3}QL_{1,1}^2$$

Washington Savannah River Company   WSRC-STI-2006-00133
Hydrogen Electrolyzer Flow Distributor Model   Revision 0
September 2006   Page 36 of 47

Fig. a6: Top row middle sub-network.

$$Q_{i+1,1}^2 - Q_{i,1}^2 + \tfrac{1}{2}QL_{i,1}\left(Q_{i,1} + Q_{i+1,1}\right) = \left(P_{i,1} - P_{i+1,1}\right)\frac{A_{slt}^2}{\mathsf{r}} - \frac{16\mathsf{m}\Delta x}{\mathsf{r}D_H^2}\left(Q_{i,1} + Q_{i+1,1}\right)$$

$$Q_{i,1} = Q_{i+1,1} + QL_{i,1}$$

$$Q_{i+1,2}^2 - Q_{i,2}^2 = \left(P_{i,2} - P_{i+1,2}\right)\frac{A_{slt}^2}{\mathsf{r}} - \frac{16\mathsf{m}\Delta x}{\mathsf{r}D_H^2}\left(Q_{i,2} + Q_{i+1,2}\right)$$

$$Q_{i,2} + QL_{i,1} + QL_{i,2} = Q_{i+1,2}$$

$$\left(P_{i,1} + P_{i+1,1}\right) - \left(P_{i,2} + P_{i+1,2}\right) = \frac{300\mathsf{m}\Delta z}{AD_p^2}\frac{\left(1-\mathsf{e}\right)^2}{\mathsf{e}^3}QL_{i,1} + \frac{3.5\mathsf{r}\Delta z}{A^2 D_p}\frac{1-\mathsf{e}}{\mathsf{e}^3}QL_{i,1}^2$$

Washington Savannah River Company
Hydrogen Electrolyzer Flow Distributor Model
September 2006

WSRC-STI-2006-00133
Revision 0
Page 37 of 47

Fig. a7: Top row exit sub-network.

$$\tfrac{1}{2}QL_{5,1}Q_{5,1} - Q_{10,1}^2 = \left(P_{5,1} - P_{6,1}\right)\frac{A_{slt}^2}{r} - \frac{16\text{m}\Delta x}{rD_H^2}Q_{5,1}$$

$$Q_{5,1} = QL_{5,1}$$

$$Q_{6,2}^2 - Q_{5,2}^2 = \left(P_{5,2} - P_{6,2}\right)\frac{A_{slt}^2}{r} - \frac{16\text{m}\Delta x}{rD_H^2}\left(Q_{5,2} + Q_{6,2}\right)$$

$$Q_{5,2} + QL_{5,1} + QL_{5,2} = Q_{6,2}$$

$$\left(P_{5,1} + P_{6,1}\right) - \left(P_{5,2} + P_{6,2}\right) = \frac{300\text{m}\Delta z}{AD_p^2}\frac{(1-\text{e})^2}{\text{e}^3}QL_{5,1} + \frac{3.5r\Delta z}{A^2 D_p}\frac{1-\text{e}}{\text{e}^3}QL_{5,1}^2$$

$$P_{out} = P_{6,2} + \frac{r}{2A_{slt}^2}\left(1 - K_{ext}\right)Q_{6,2}^2$$

Washington Savannah River Company
Hydrogen Electrolyzer Flow Distributor Model
September 2006
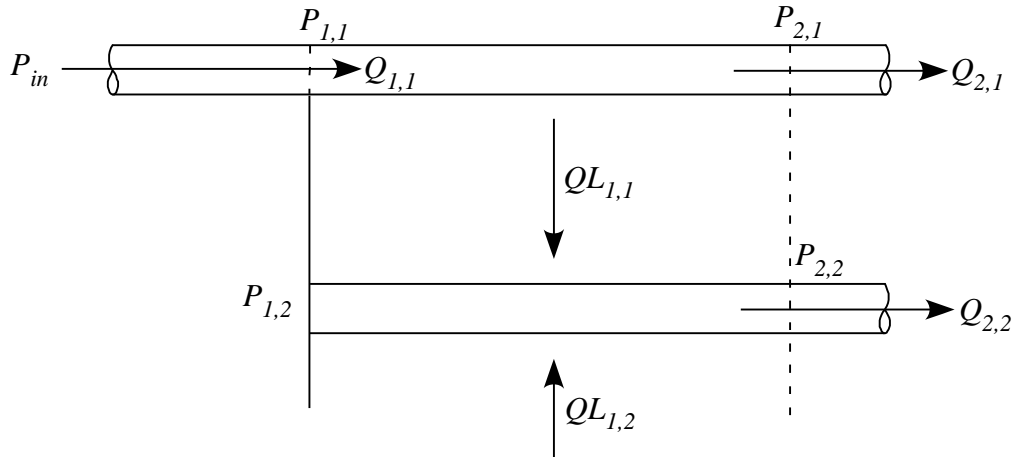
WSRC-STI-2006-00133
Revision 0
Page 38 of 47
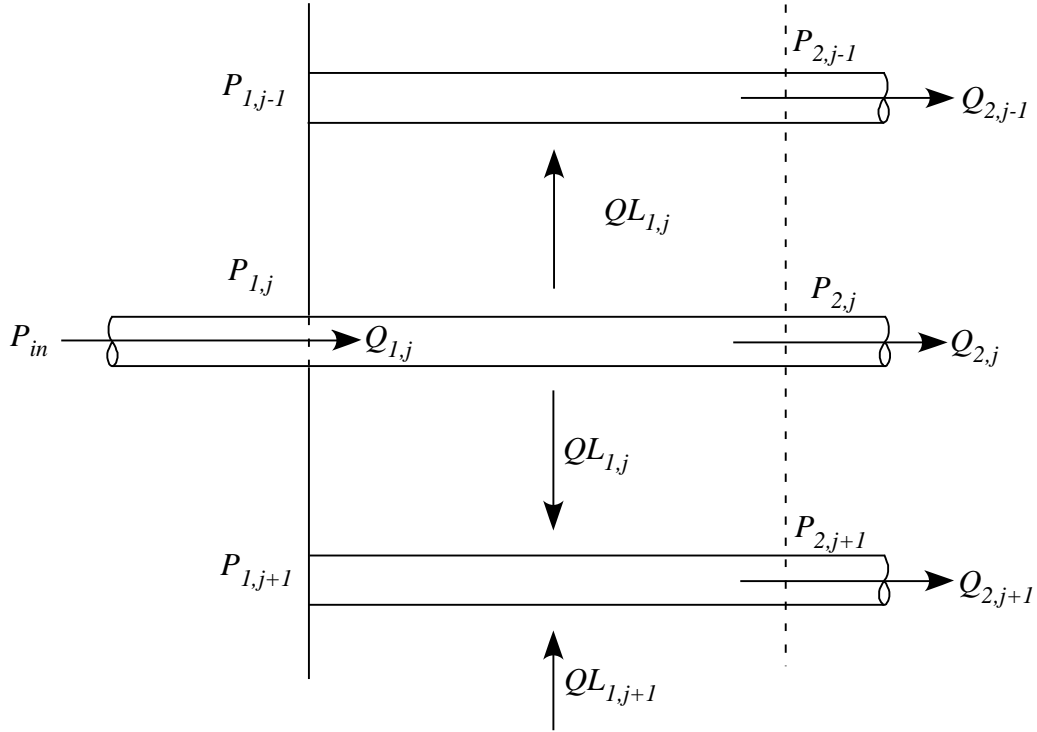
Fig. a8: Middle row entrance sub-network.

$$P_{in} = P_{1,j} + \frac{r}{2A_{slt}^2}\left(1 + K_{ent}\right)Q_{1,j}^2$$

$$Q_{2,j}^2 - Q_{1,j}^2 + \tfrac{1}{2}\left(QL_{1,j-1} + QL_{1,j}\right)\left(Q_{1,j} + Q_{2,j}\right) = \left(P_{1,j} - P_{2,j}\right)\frac{A_{slt}^2}{r} - \frac{16m\Delta x}{rD_H^2}\left(Q_{1,j} + Q_{2,j}\right)$$

$$Q_{1,j} = Q_{2,j} + QL_{1,j-1} + QL_{1,j}$$

$$Q_{2,j+1}^2 = \left(P_{1,j+1} - P_{2,j+1}\right)\frac{A_{slt}^2}{r} - \frac{16m\Delta x}{rD_H^2}Q_{2,j+1}$$

$$QL_{1,j} + QL_{1,j+1} = Q_{2,j+1}$$

$$\left(P_{1,j} + P_{2,j}\right) - \left(P_{1,j+1} + P_{2,j+1}\right) = \frac{300m\Delta z}{AD_p^2}\frac{(1-e)^2}{e^3}QL_{1,j} + \frac{3.5r\Delta z}{A^2 D_p}\frac{1-e}{e^3}QL_{1,j}^2$$
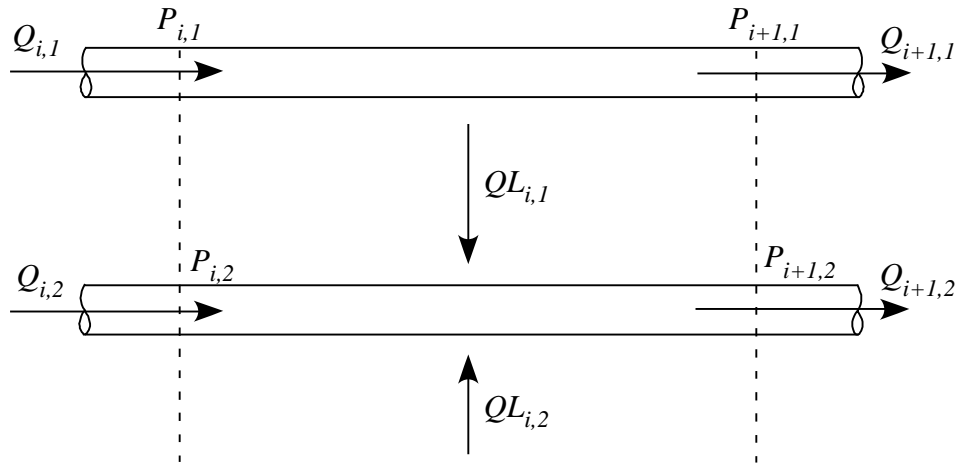
$$\left(P_{1,j} + P_{2,j}\right) - \left(P_{1,j-1} + P_{2,j-1}\right) = \frac{300m\Delta z}{AD_p^2}\frac{(1-e)^2}{e^3}QL_{1,j-1} + \frac{3.5r\Delta z}{A^2 D_p}\frac{1-e}{e^3}QL_{1,j-1}^2$$
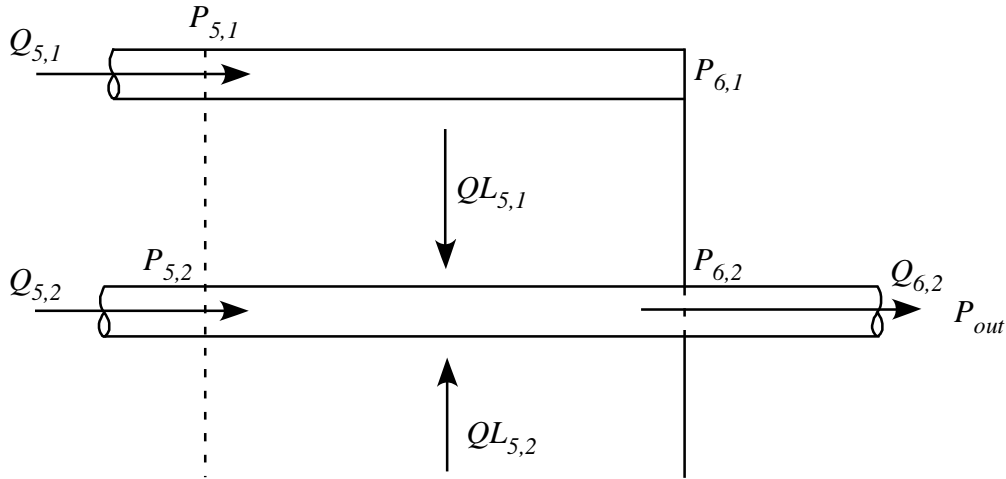
Washington Savannah River Company   WSRC-STI-2006-00133
Hydrogen Electrolyzer Flow Distributor Model   Revision 0
September 2006   Page 39 of 47
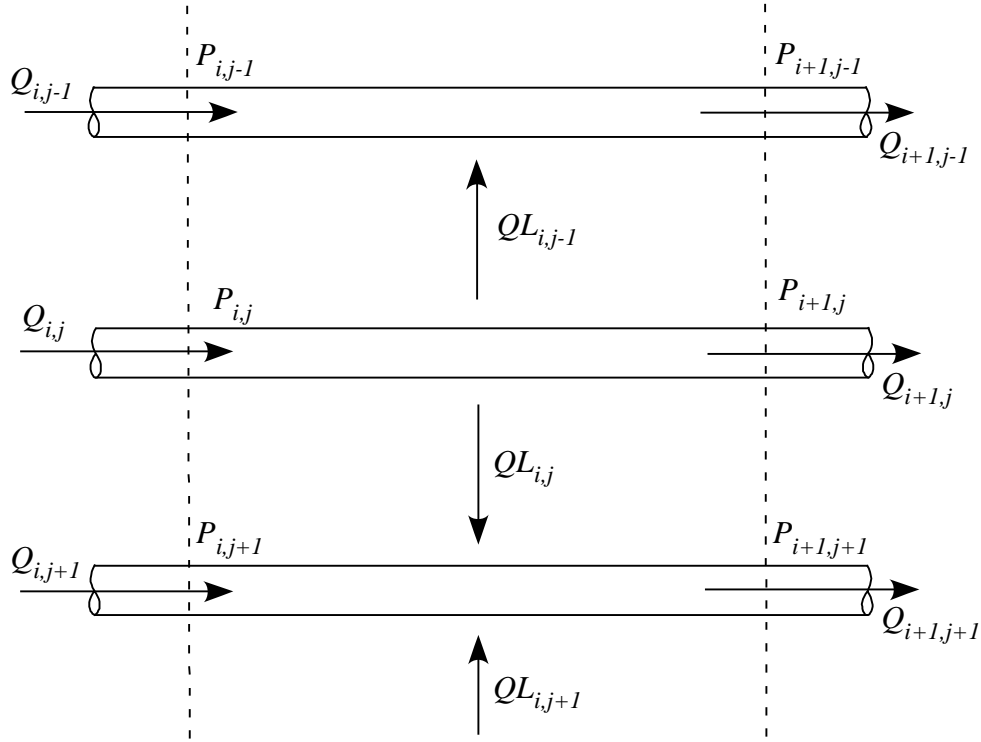
Fig. a9: Middle row middle sub-network.

$$Q_{i+1,j}^2 - Q_{i,j}^2 + \tfrac{1}{2}\left(QL_{i,j-1} + QL_{i,j}\right)\left(Q_{i,j} + Q_{i+1,j}\right) = \left(P_{i,j} - P_{i+1,j}\right)\frac{A_{slt}^2}{\mathsf{r}} - \frac{16\mathsf{m}\Delta x}{\mathsf{r}D_H^2}\left(Q_{i,j} + Q_{i+1,j}\right)$$

$$Q_{i,j} = Q_{i+1,j} + QL_{i,j-1} + QL_{i,j}$$

$$Q_{i+1,j+1}^2 - Q_{i,j+1}^2 = \left(P_{i,j+1} - P_{i+1,j+1}\right)\frac{A_{slt}^2}{\mathsf{r}} - \frac{16\mathsf{m}\Delta x}{\mathsf{r}D_H^2}\left(Q_{i,j+1} + Q_{i+1,j+1}\right)$$

$$Q_{i,j+1} + QL_{i,j} + QL_{i,j+1} = Q_{i+1,j+1}$$

$$\left(P_{i,j} + P_{i+1,j}\right) - \left(P_{i,j-1} + P_{i+1,j-1}\right) = \frac{300\mathsf{m}\Delta z}{AD_p^2}\frac{(1-\mathsf{e})^2}{\mathsf{e}^3}QL_{i,j-1} + \frac{3.5\mathsf{r}\Delta z}{A^2 D_p}\frac{1-\mathsf{e}}{\mathsf{e}^3}QL_{i,j-1}^2$$

$$\left(P_{i,j} + P_{i+1,j}\right) - \left(P_{i,j+1} + P_{i+1,j+1}\right) = \frac{300\mathsf{m}\Delta z}{AD_p^2}\frac{(1-\mathsf{e})^2}{\mathsf{e}^3}QL_{i,j} + \frac{3.5\mathsf{r}\Delta z}{A^2 D_p}\frac{1-\mathsf{e}}{\mathsf{e}^3}QL_{i,j}^2$$

Washington Savannah River Company   WSRC-STI-2006-00133
Hydrogen Electrolyzer Flow Distributor Model   Revision 0
September 2006   Page 40 of 47
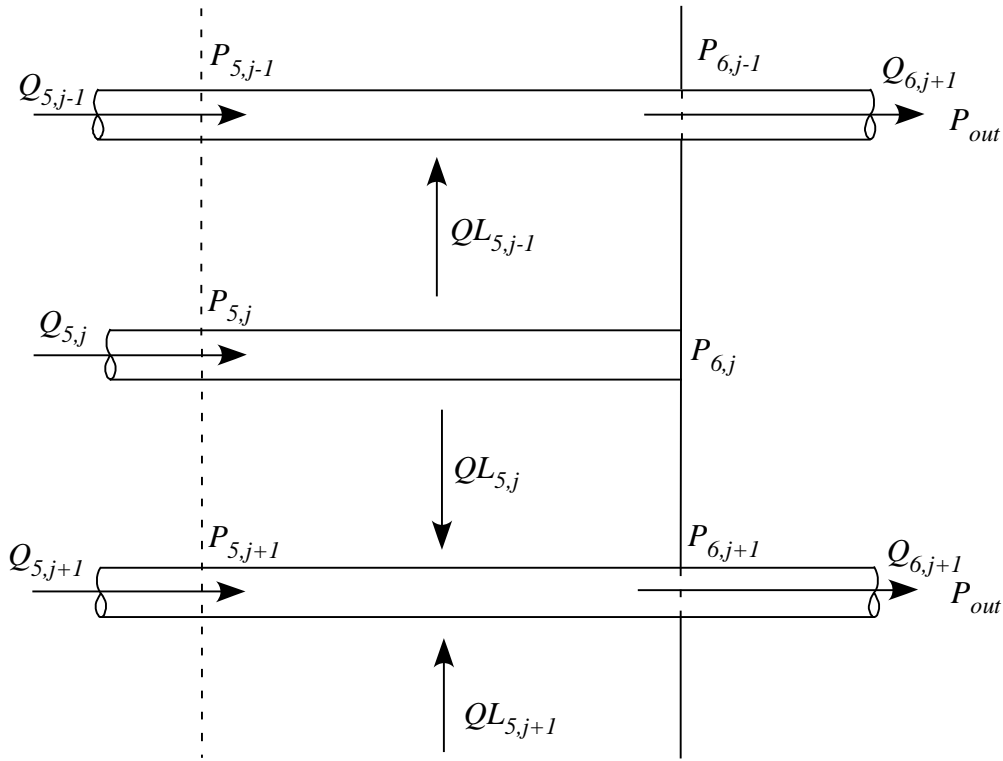
Fig. a10: Middle row exit sub-network.

$$\tfrac{1}{2}\left(QL_{5,j-1}+QL_{5,j}\right)Q_{5,j}-Q_{5,j}^2=\left(P_{5,j}-P_{6,j}\right)\frac{A_{slt}^2}{r}-\frac{16\mathrm{m}\Delta x}{rD_H^2}Q_{5,j}$$

$$Q_{5,j}=QL_{5,j}+QL_{5,j-1}$$

$$Q_{6,j+1}^2-Q_{5,j+1}^2=\left(P_{5,j+1}-P_{6,j+1}\right)\frac{A_{slt}^2}{r}-\frac{16\mathrm{m}\Delta x}{rD_H^2}\left(Q_{5,j+1}+Q_{6,j+1}\right)$$

$$Q_{5,j+1}+QL_{5,j}+QL_{5,j+1}=Q_{6,j+1}$$

$$\left(P_{5,j}+P_{6,j}\right)-\left(P_{5,j-1}+P_{6,j-1}\right)=\frac{300\mathrm{m}\Delta z}{AD_p^2}\frac{(1-\mathrm{e})^2}{\mathrm{e}^3}QL_{5,j-1}+\frac{3.5\mathrm{r}\Delta z}{A^2D_p}\frac{1-\mathrm{e}}{\mathrm{e}^3}QL_{5,j-1}^2$$

$$\left(P_{5,j}+P_{6,j}\right)-\left(P_{5,j+1}+P_{6,j+1}\right)=\frac{300\mathrm{m}\Delta z}{AD_p^2}\frac{(1-\mathrm{e})^2}{\mathrm{e}^3}QL_{5,j}+\frac{3.5\mathrm{r}\Delta z}{A^2D_p}\frac{1-\mathrm{e}}{\mathrm{e}^3}QL_{5,j}^2$$

$$P_{out}=P_{6,j+1}+\frac{\mathrm{r}}{2A_{slt}^2}\left(1-K_{ext}\right)Q_{6,j+1}^2$$
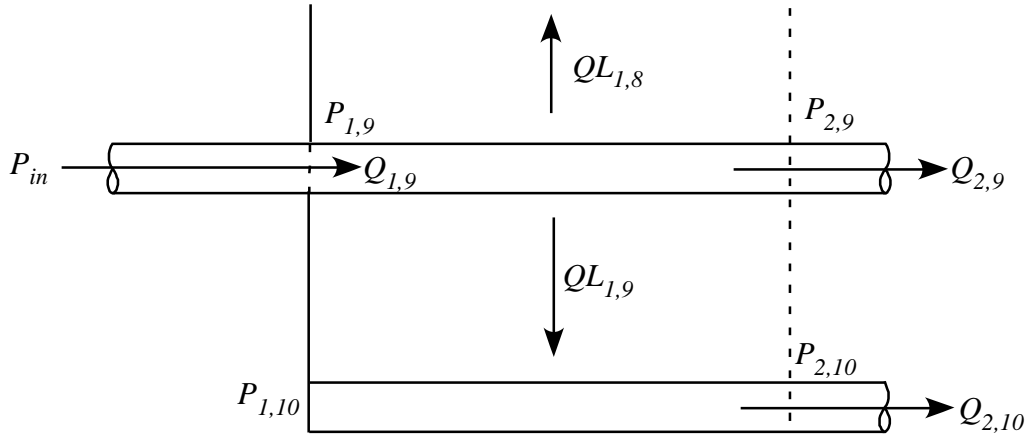
Fig. a11: Bottom row entrance sub-network.

$$P_{in} = P_{1,9} + \frac{r}{2A_{slt}^2}\left(1 + K_{ent}\right)Q_{1,9}^2$$

$$Q_{2,9}^2 - Q_{1,9}^2 + \tfrac{1}{2}\left(QL_{1,8} + QL_{1,9}\right)\left(Q_{1,9} + Q_{2,9}\right) = \left(P_{1,9} - P_{2,9}\right)\frac{A_{slt}^2}{r} - \frac{16m\Delta x}{rD_H^2}\left(Q_{1,9} + Q_{2,9}\right)$$

$$Q_{1,9} = Q_{2,9} + QL_{1,8} + QL_{1,9}$$

$$Q_{2,10}^2 = \left(P_{1,10} - P_{2,10}\right)\frac{A_{slt}^2}{r} - \frac{16m\Delta x}{rD_H^2}Q_{2,10}$$

$$QL_{1,9} = Q_{2,10}$$

$$\left(P_{1,9} + P_{2,9}\right) - \left(P_{1,8} + P_{2,8}\right) = \frac{300m\Delta z}{AD_p^2}\frac{\left(1-e\right)^2}{e^3}QL_{1,8} + \frac{3.5r\Delta z}{A^2 D_p}\frac{1-e}{e^3}QL_{1,8}^2$$

$$\left(P_{1,9} + P_{2,9}\right) - \left(P_{1,10} + P_{2,10}\right) = \frac{300m\Delta z}{AD_p^2}\frac{\left(1-e\right)^2}{e^3}QL_{1,9} + \frac{3.5r\Delta z}{A^2 D_p}\frac{1-e}{e^3}QL_{1,9}^2$$
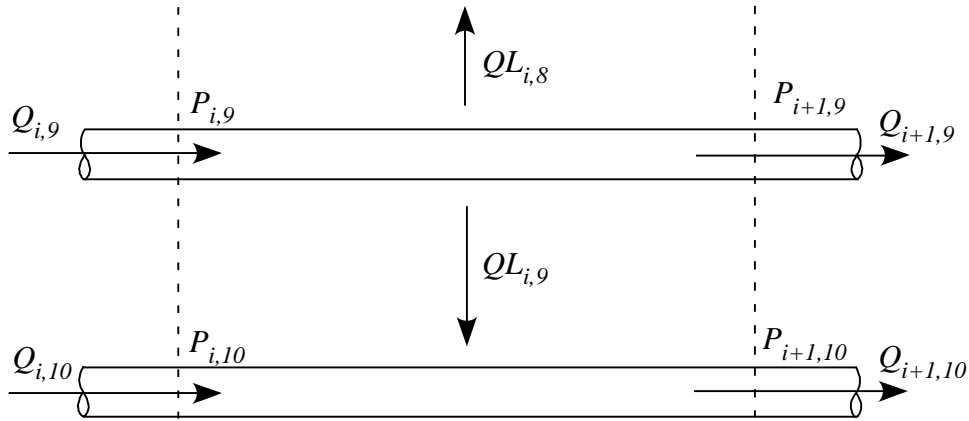
Washington Savannah River Company   WSRC-STI-2006-00133
Hydrogen Electrolyzer Flow Distributor Model   Revision 0
September 2006   Page 42 of 47

Fig. a12: Bottom row middle sub-network.

$$Q_{i+1,9}^2 - Q_{i,9}^2 + \tfrac{1}{2}\left(QL_{i,8} + QL_{i,9}\right)\left(Q_{i,9} + Q_{i+1,9}\right) = \left(P_{i,9} - P_{i+1,9}\right)\frac{A^2}{\mathsf{r}} - \frac{16\mathsf{m}\Delta x}{\mathsf{r}D_H^2}\left(Q_{i,9} + Q_{i+1,9}\right)$$

$$Q_{i,9} = QL_{i,8} + QL_{i,9} + Q_{i+1,9}$$

$$Q_{i+1,10}^2 - Q_{i,10}^2 = \left(P_{i,10} - P_{i+1,10}\right)\frac{A^2}{\mathsf{r}} - \frac{16\mathsf{m}\Delta x}{\mathsf{r}D_H^2}\left(Q_{i,10} + Q_{i+1,10}\right)$$

$$Q_{i,10} + QL_{i,9} = Q_{i+1,10}$$

$$\left(P_{i,9} + P_{i+1,9}\right) - \left(P_{i,8} + P_{i+1,8}\right) = \frac{300\mathsf{m}\Delta z}{AD_p^2}\frac{\left(1-\mathsf{e}\right)^2}{\mathsf{e}^3}QL_{i,8} + \frac{3.5\mathsf{r}\Delta z}{A^2 D_p}\frac{1-\mathsf{e}}{\mathsf{e}^3}QL_{i,8}^2$$

$$\left(P_{i,9} + P_{i+1,9}\right) - \left(P_{i,10} + P_{i+1,10}\right) = \frac{300\mathsf{m}\Delta z}{AD_p^2}\frac{\left(1-\mathsf{e}\right)^2}{\mathsf{e}^3}QL_{i,9} + \frac{3.5\mathsf{r}\Delta z}{A^2 D_p}\frac{1-\mathsf{e}}{\mathsf{e}^3}QL_{i,9}^2$$

Washington Savannah River Company
Hydrogen Electrolyzer Flow Distributor Model
September 2006

WSRC-STI-2006-00133
Revision 0
Page 43 of 47

Fig. a13: Bottom row exit sub-network.

$$\tfrac{1}{2}\left(QL_{5,8} + QL_{5,9}\right)Q_{5,9} - Q_{5,9}^2 = \left(P_{5,9} - P_{6,9}\right)\frac{A_{slt}^2}{r} - \frac{16m\Delta x}{rD_H^2}Q_{5,9}$$

$$Q_{5,9} = QL_{5,8} + QL_{5,9}$$

$$Q_{6,10}^2 - Q_{5,10}^2 = \left(P_{5,10} - P_{6,10}\right)\frac{A_{slt}^2}{r} - \frac{16m\Delta x}{rD_H^2}\left(Q_{5,10} + Q_{6,10}\right)$$

$$Q_{5,10} + QL_{5,9} = Q_{6,10}$$

$$\left(P_{5,9} + P_{6,9}\right) - \left(P_{5,8} + P_{6,8}\right) = \frac{300m\Delta z}{AD_p^2}\frac{\left(1-e\right)^2}{e^3}QL_{5,8} + \frac{3.5r\Delta z}{A^2D_p}\frac{1-e}{e^3}QL_{5,8}^2$$

$$\left(P_{5,9} + P_{6,9}\right) - \left(P_{5,10} + P_{6,10}\right) = \frac{300m\Delta z}{AD_p^2}\frac{\left(1-e\right)^2}{e^3}QL_{5,9} + \frac{3.5r\Delta z}{A^2D_p}\frac{1-e}{e^3}QL_{5,9}^2$$
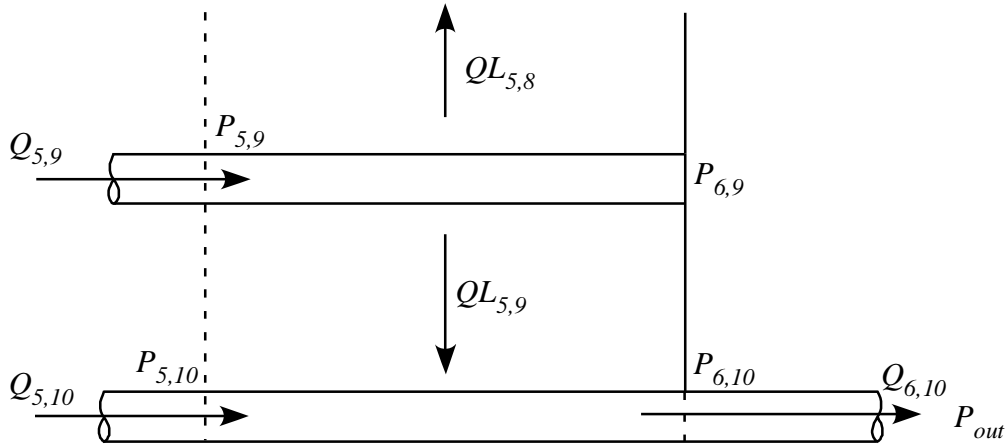
$$P_{out} = P_{6,10} + \frac{r}{2A_2}\left(1-K_{ext}\right)Q_{6,10}^2$$

Washington Savannah River Company
Hydrogen Electrolyzer Flow Distributor Model
September 2006

WSRC-STI-2006-00133
Revision 0
Page 44 of 47

This Page Deliberately Left Blank

Appendix B Analytical Channel Pressure Distributions

As part of the code validation effort, analytical solutions for the pressure distributions in the supply and exhaust channels of the flow distributor were obtained for comparison with model results. Figure b1 is a schematic of a channel with axial flow and uniform flow out of the bottom of the channel. Also shown is an incremental control volume in the channel.
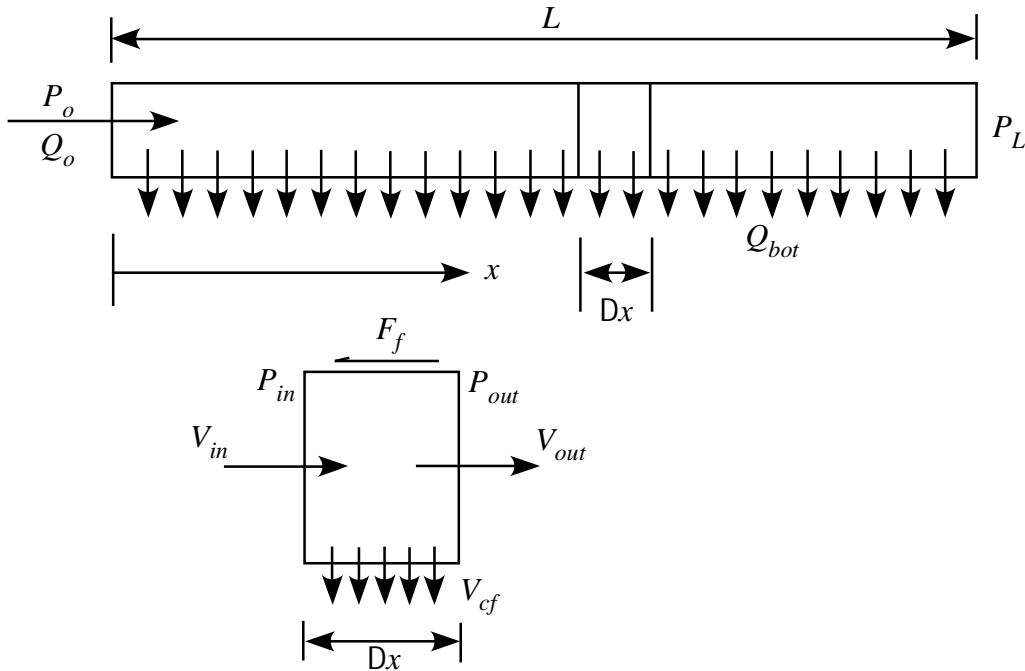

Fig. b1: Schematic of axial flow through a channel with uniform flow out through the bottom of the channel.

Equation (b1) is the linear momentum equation for axial flow through the incremental control volume in figure b1. The flow is assumed to be laminar and equation (b2) is the expression for the wall drag. The mass flowrates are expressed in terms of the velocity in equation (b3). Equation (b4) is the simplified form of this equation. Taking the limit • x• 0 of equation (b4) results in the differential equation (b5). Equation (b6) shows the expressions for the axial velocity and the velocity gradient. Substituting these expressions into the differential equation results in equation (b7). The differential equation is integrated as shown in equation (b8), and the final solution is equation (b9). This is equation (8).

$$\dot{m}_{out} V_{out} + \dot{m}_{cf} \tfrac{1}{2}(V_{in} + V_{out}) - \dot{m}_{in} V_{in} = (P_{in} - P_{out})A_{slt} - F_f \qquad (b1)$$

Washington Savannah River Company
Hydrogen Electrolyzer Flow Distributor Model
September 2006

WSRC-STI-2006-00133
Revision 0
Page 46 of 47

$$F_f = \frac{32 A_{slt} \Delta x \dot{m} \overline{V}}{D_H^2} \tag{b2}$$

$$r A_{slt} V_{out}^2 + r A_{slt} (V_{in} - V_{out}) \overline{V} - r A_{slt} V_{in}^2 = (P_{in} - P_{out}) A_{slt} - \frac{32 A_{slt} \Delta x \dot{m}}{D_H^2} \overline{V} \tag{b3}$$

$$\frac{P_{out} - P_{in}}{\Delta x} = -r \overline{V} \left(\frac{V_{out} - V_{in}}{\Delta x} \right) - \frac{32 \dot{m}}{D_H^2} \overline{V} \tag{b4}$$

$$\frac{dp}{dx} = -r V \frac{dV}{dx} - \frac{32 \dot{m}}{D_H^2} V \tag{b5}$$

$$V = V_0 \left(1 - \frac{x}{L} \right) \quad \& \quad \frac{dV}{dx} = -\frac{V_0}{L} \tag{b6}$$

$$\frac{dP}{dx} = \left(r \frac{V_0}{L} - \frac{32 \dot{m}}{D_H^2} \right) V_0 \left(1 - \frac{x}{L} \right) \tag{b7}$$

where: $P = P_0$ @ $x = 0$

$$P - P_0 = V_0 \left(r \frac{V_0}{L} - \frac{32 \dot{m}}{D_H^2} \right) \int_0^x \left(1 - \frac{a}{L} \right) da \tag{b8}$$

$$P(x) = P_0 + V_0 \left(r \frac{V_0}{L} - \frac{32 \dot{m}}{D_H^2} \right) \left(x - \frac{x^2}{2L} \right) \tag{b9}$$

Figure b2 is a schematic of a channel with axial flow and uniform flow into the bottom of the channel. Also shown is an incremental control volume in the channel. Equation (b10) is the linear momentum equation for the axial flow through the incremental control volume. There is not a momentum rate term involving the upflow through the channel bottom, because this flow enters the control volume with no axial momentum. The differential equation is derived in the same manner as in the previous derivation. Equation (b14 is the final form of the differential equation and the boundary condition. Equation (b15) is the solution, and it is also equation (10).
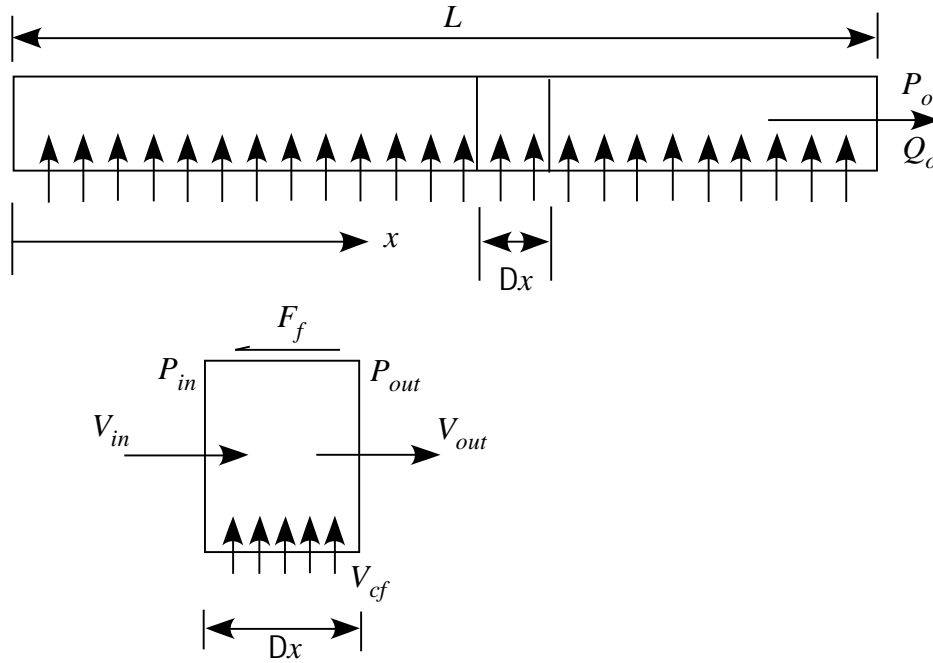
Washington Savannah River Company
Hydrogen Electrolyzer Flow Distributor Model
September 2006

WSRC-STI-2006-00133
Revision 0
Page 47 of 47

Fig. b2: Schematic of axial flow through a channel with uniform flow in through the bottom of the channel.

$$\dot{m}_{out}V_{out} - \dot{m}_{in}V_{in} = (P_{in} - P_{out})A_{slt} - F_f \tag{b10}$$

$$2\rho(V_{out} - V_{in})\overline{V} = P_{in} - P_{out} - \frac{32\mu\Delta x}{D_H^2}\overline{V} \tag{b11}$$

$$2\rho V\frac{dV}{dx} = -\frac{dP}{dx} - \frac{32\mu}{D_H^2}V \tag{b12}$$

$$V = V_0\frac{x}{L} \qquad \& \qquad \frac{dV}{dx} = \frac{V_0}{L} \tag{b13}$$

$$\frac{dP}{dx} = -\left(\frac{2\rho V_0}{L} + \frac{32\mu}{D_H^2}\right)\frac{x}{L}V_0 \tag{b14}$$

where: $P = P_0$ @ $x = L$

$$P(x) = P_0 + \frac{V_0}{2L}\left(\frac{2\rho V_0}{L} + \frac{32\mu}{D_H^2}\right)(L^2 - x^2) \tag{b15}$$